



Elettra  
Sincrotrone  
Trieste

# Synchrotron Radiation for biomedical imaging

*Giuliana Tromba*

**SYnchrotron Radiation for MEDical Physics (SYRMEP) beamline**

*Elettra - Sincrotrone Trieste*

XVI International Conference  
on Science, Arts and Culture

International Conference

ON

**SESAME**

In Honour of Paolo Budinich

29 August - 2 September 2016

Veli Lošinj, Croatia



**ECSCAC**

EUROPEAN CENTRE  
FOR SCIENCE ARTS AND  
CULTURE



# Outline

- Advantages of using SR for medical applications
- SR *phase contrast* imaging
- Some applications at ESRF, Spring8, Elettra
  - Mammography
  - Studies of bones, joints and cartilages
  - Lungs imaging
  - Brain studies
  - Imaging of atherosclerotic plaques
  - .....
- Final considerations



## **Monochromaticity** allows for:

- *optimization* of X-ray energy according to the specific case under study (dose reduction)
- quantitative CT evaluations
- no beam hardening
- convenient use of contrast agent (K-edge and L-edge imaging)

## **Spatial coherence** enables the applications of *phase sensitive imaging techniques*

- Phase contrast overcomes the limitation of conventional radiology
- It brings to a dose reduction
- Improved contrast resolution, edges enhancement
- Use of phase retrieval algorithms

## **High fluxes**

- Short exposure time
- Dynamic studies....

## **Collimation**

- parallel beams, scatter reduction
- beam shaping (micro-beams)



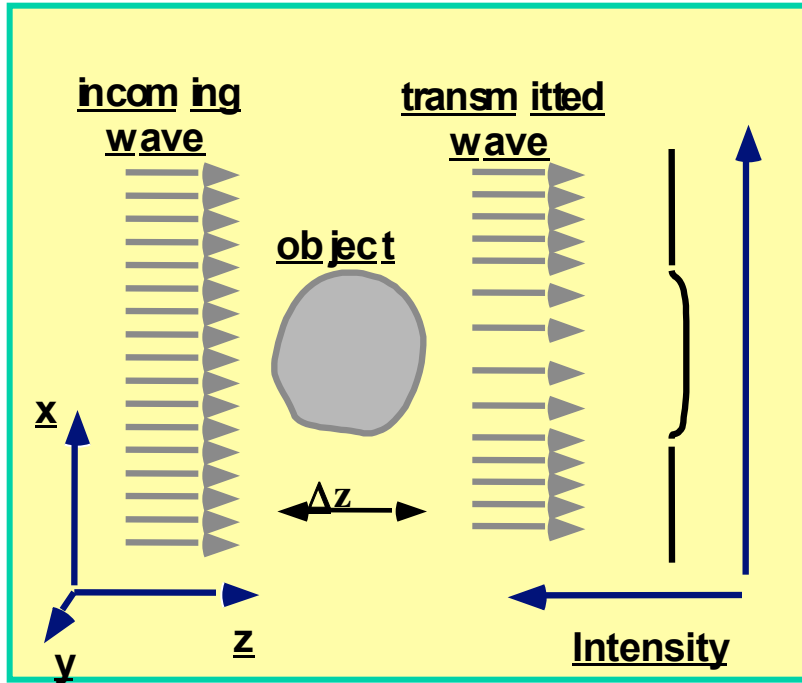
# Imaging approaches

- Clinical: applications to patients  
(es. angiography, mammography, ecc.)  
*Need to **limit** radiation dose. Find best compromise between dose and image quality*
- Imaging of small animals: applied for different purposes in the development of **animal models**  
(es. Cell tracking, Osteoporosis, genetic diseases,...)  
*Research protocols, control of dose.*
- “In vitro” imaging: it concerns the study of biological samples. (es. micro-tomography applied on bone samples, scaffolds, cartilages, etc.)  
*Requirements of high resolution and high sensitivity*

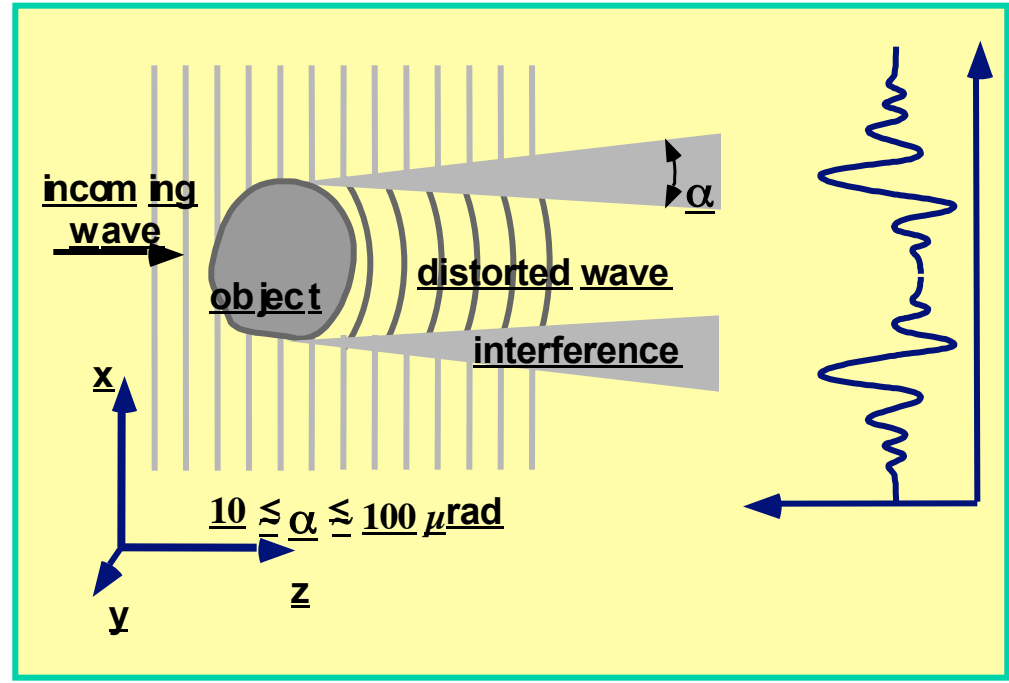


Increase of dose and spatial resolution

# PHase Contrast (PHC) vs. absorption contrast



Absorption radiology (conventional)



PHC

In **conventional radiology** image formation is based on differences in X-ray absorption properties of the samples. The image contrast is generated by density, composition or thickness variation of the sample. Main limitation: **poor contrast in soft tissue differentiation**. **Phase contrast techniques** are based on the observation of the *phase shifts* produced by the object on the incoming wave. Contrast arises from interference among parts of the wave front differently deviated (or phase shifted) by the sample. Edge enhancement effects.

**Refraction index for hard X-rays** :  $n = 1 - \delta + i\beta$ ,  $\beta$  = absorption term,  $\delta$  = phase shift term  
for soft tissue@17 keV:  $\beta \sim 10^{-10}$ ;  $\delta \sim 10^{-6}$ ,  $\delta \propto \lambda^2$ ,  $\beta \propto \lambda^3$

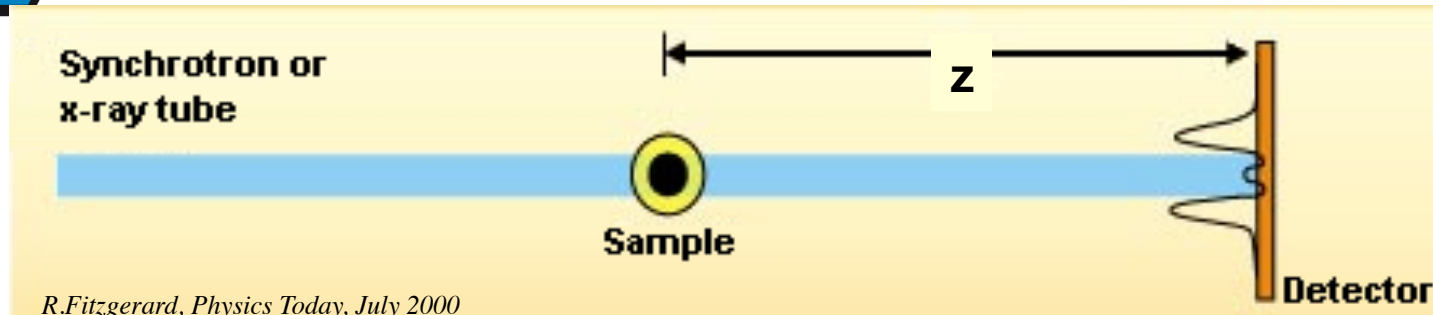
**Absorption radiology** -> contrast is generated by differences in the x-ray absorption ( $C_{abs} \sim x \Delta\beta$ ),

**Phase Radiology** -> contrast is generated by phase shifts ( $C_{\phi} \sim x \Delta\delta$ )

$x$  = object size // to beam direction

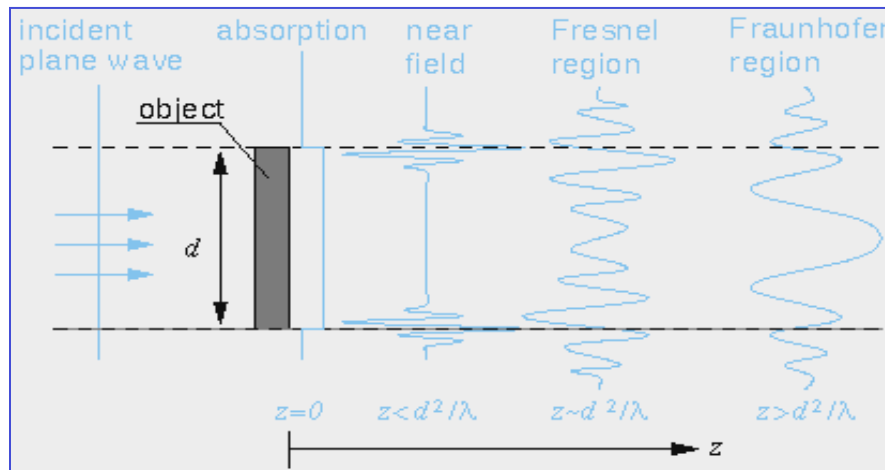
$\delta \gg \beta \rightarrow$  phase shifts effects  $\gg$  absorption

# Propagation based imaging (PBI)



- The technique exploits the high spatial coherence of the X-ray source.
- $z = 0$  -> absorption image
- For  $z > 0$  -> interference between diffracted and un-diffracted wave produces edge and contrast enhancement. A variation of  $\delta$  is detected
- Measure of  $\nabla^2\Phi(x,y)$
- The technique requires a high spatial coherence source and detectors with adequate spatial resolution. Monochromaticity is not needed
- Phase effects visible also at low dose (mammography trial @ SYRMEP)

Regimes

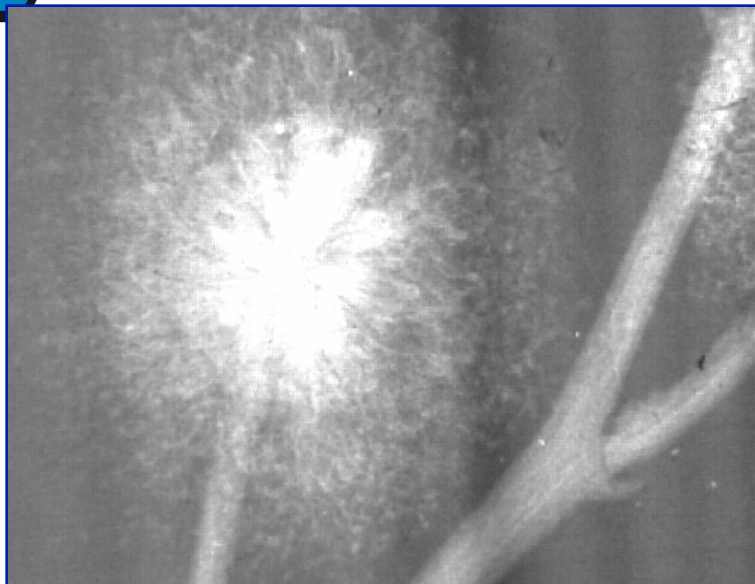


Snigirev A. et al., *Rev. Sci. Instrum.* 66, 1995  
 Wilkins S. W. et al., *Nature* 384, 1996  
 Cloetens P. et al., *J. Phys D: Appl. Phys.* 29, 1996  
 Arfelli F et al., *Phys. Med. Biol.* 43, 1998

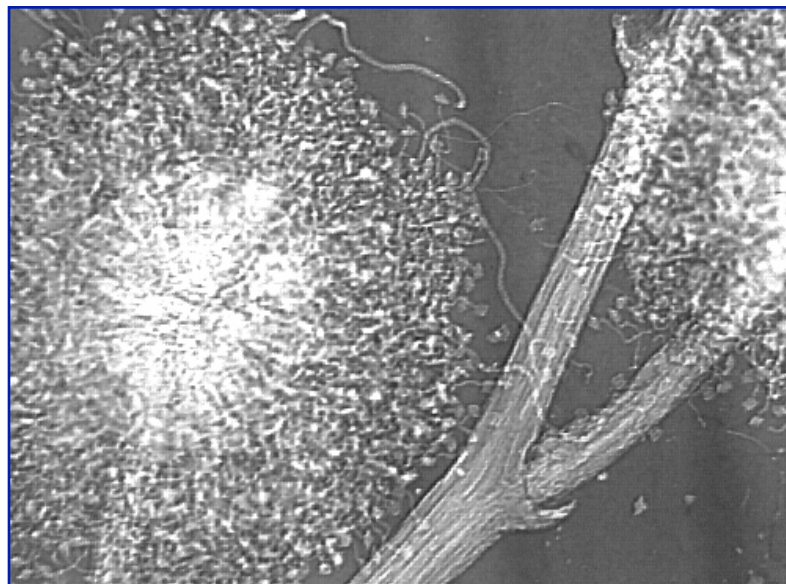


# Imaging a Mimosa flower....

10 keV

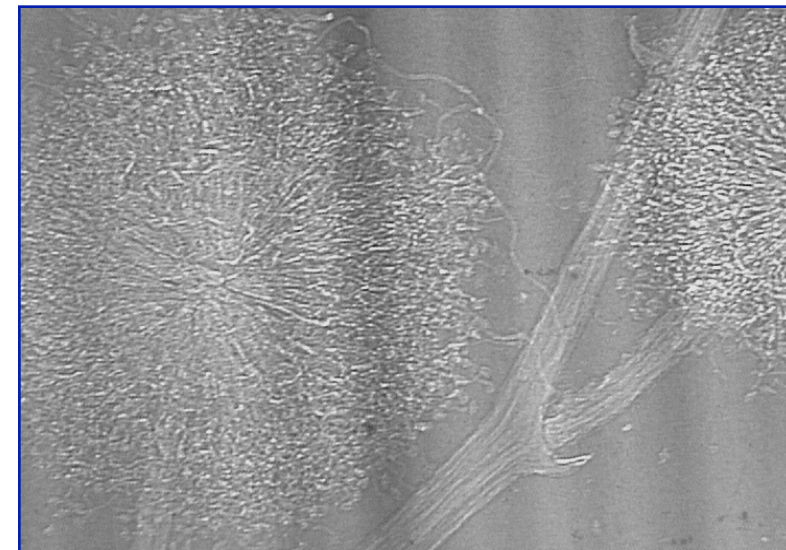
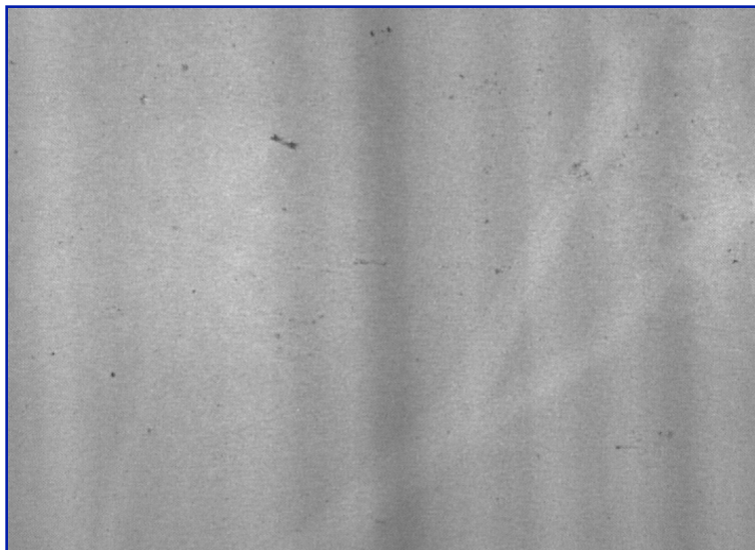


Absorption

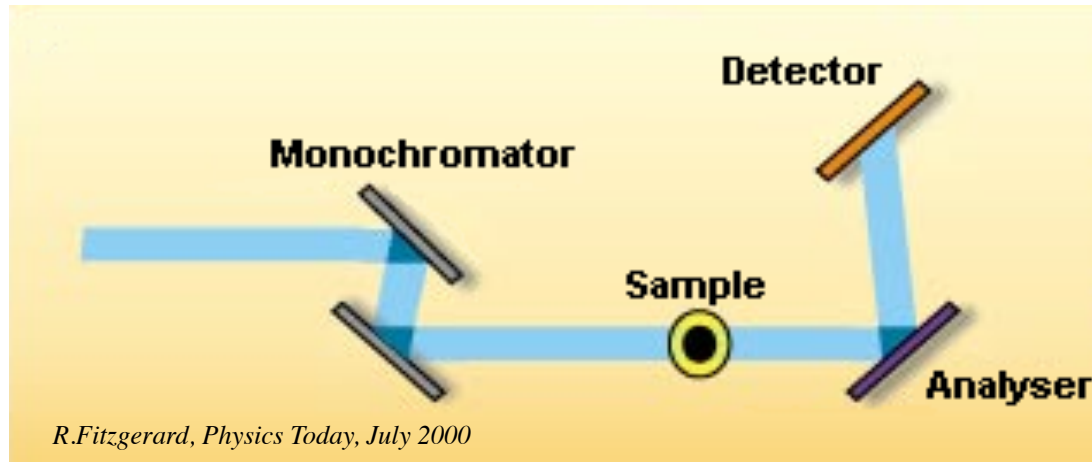


PBI

25 keV



# Analyzer Based Imaging (ABI)



- Sensitive to refraction of X-rays
- A perfect crystal is used as an angular filter to select angular emission of X-rays. The filtering function is the rocking curve (FWHM: 1-20  $\mu\text{rad}$ )
- Image formation with ABI is sensitive to a variation of  $\delta$  in the sample. Indeed, **refraction angle is roughly proportional to the gradient of  $\delta$**
- Analyzer and monochromator aligned  $\rightarrow$  X-ray scattered by more than some tens  $\mu\text{rad}$  are rejected
- Small misalignments  $\rightarrow$  investigation of phase shift effects
- With greater misalignments the primary beam is almost totally rejected and pure refraction images are obtained
- Sensitive to  $\nabla\Phi(x,y)$
- The technique requires the beam monochromaticity, spatial coherence is less stringent.

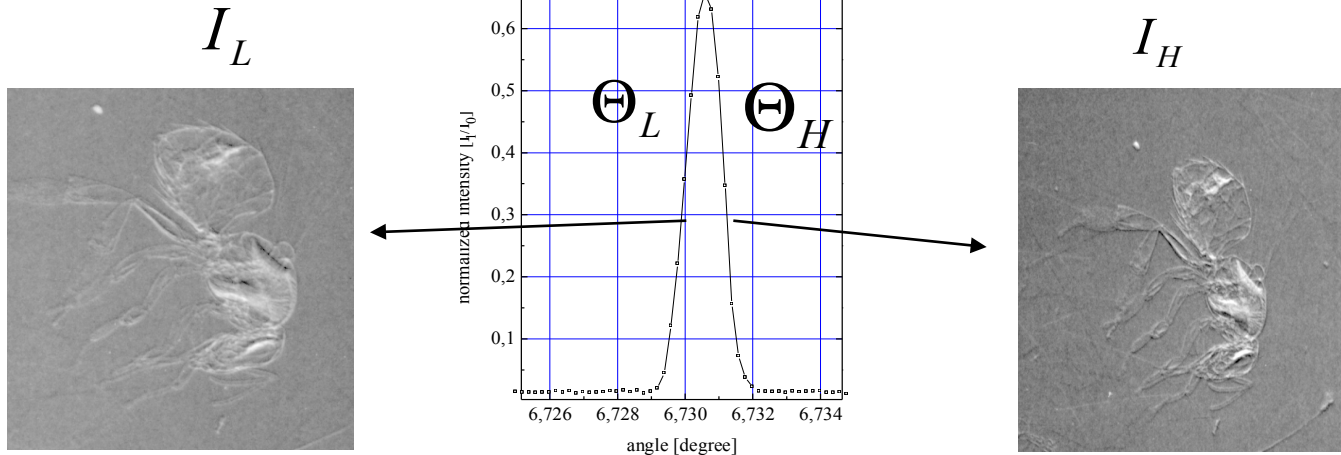
*Podurets K. M. et al., Sov. Phys. Tech. Phys. 34(6), 1989*

*V. N. Ingal and E. A. Beliaevskaya, J. Phys. D: Appl. Phys. 28, 1995*

*Chapman D et al., Phys. Med. Biol. 42, 1997*



# ABI image manipulation (original algorithm)



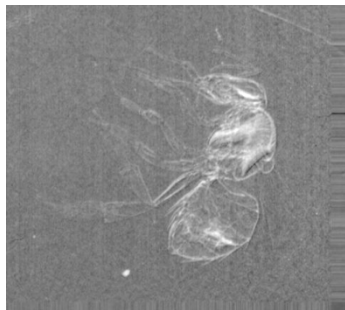
Linear approximation of rocking curve at half values ( $I_R$  and  $I_L$ )

$$I_L = I_R \left( R(\Theta_L) + \frac{\partial R}{\partial \Theta}(\Theta_L) \Delta \Theta_z \right)$$

$$I_H = I_R \left( R(\Theta_H) + \frac{\partial R}{\partial \Theta}(\Theta_H) \Delta \Theta_z \right)$$

$\Theta_z$  = refraction Image

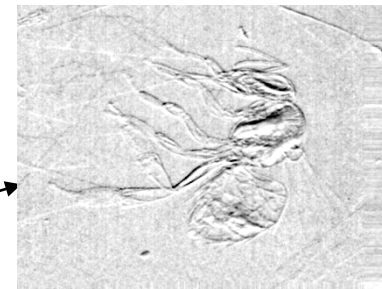
$I_R$  = apparent absorption image (absorption + extinction)



Apparent Absorption Image

$$I_R = \frac{I_L \cdot \frac{dR}{d\Theta} \Big|_{\Theta_H} - I_H \cdot \frac{dR}{d\Theta} \Big|_{\Theta_L}}{R(\Theta_L) \cdot \frac{dR}{d\Theta} \Big|_{\Theta_H} - R(\Theta_H) \cdot \frac{dR}{d\Theta} \Big|_{\Theta_L}}$$

$$\Theta_z = \frac{I_H \cdot R(\Theta_L) - I_L \cdot R(\Theta_H)}{I_L \cdot \frac{dR}{d\Theta} \Big|_{\Theta_H} - I_H \cdot \frac{dR}{d\Theta} \Big|_{\Theta_L}}$$

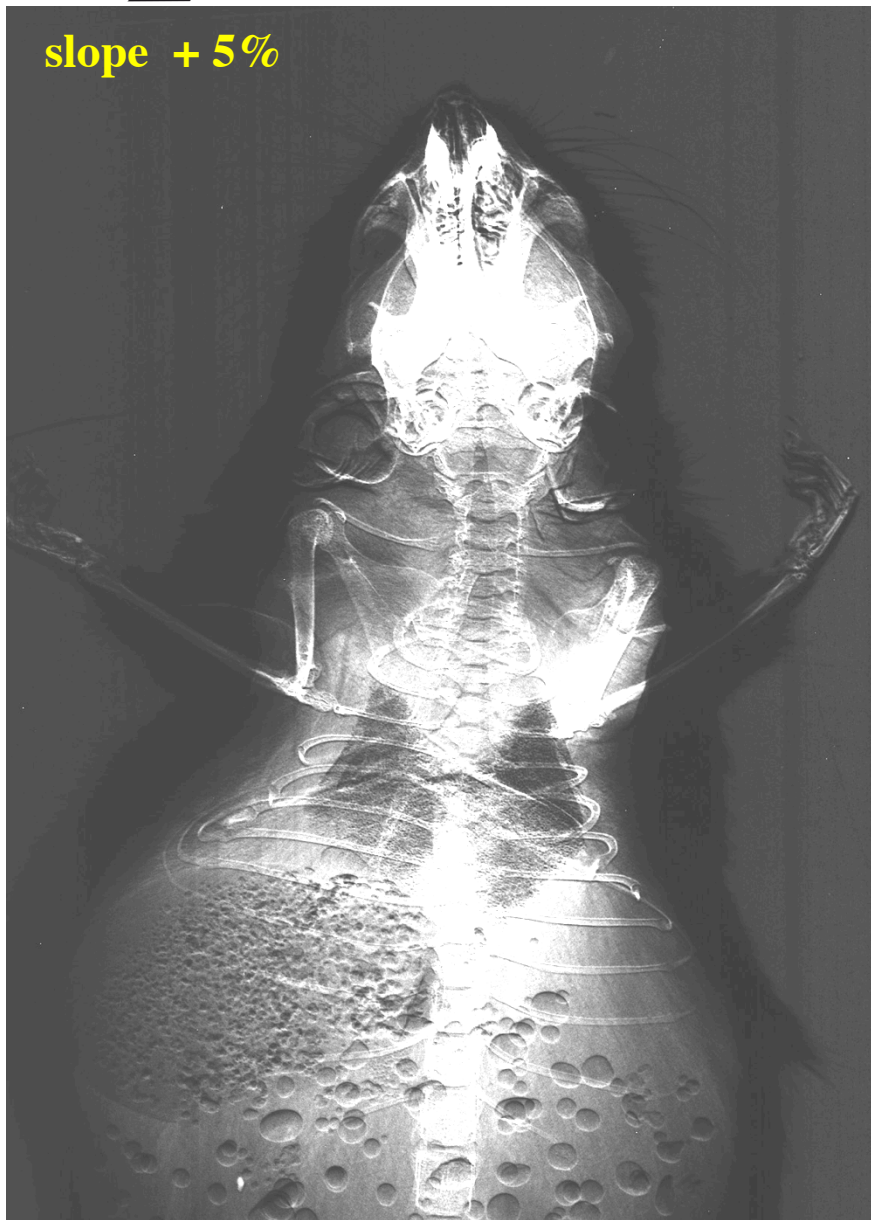


Refraction Image



# ABI images for different analyzer positions

slope + 5%



top



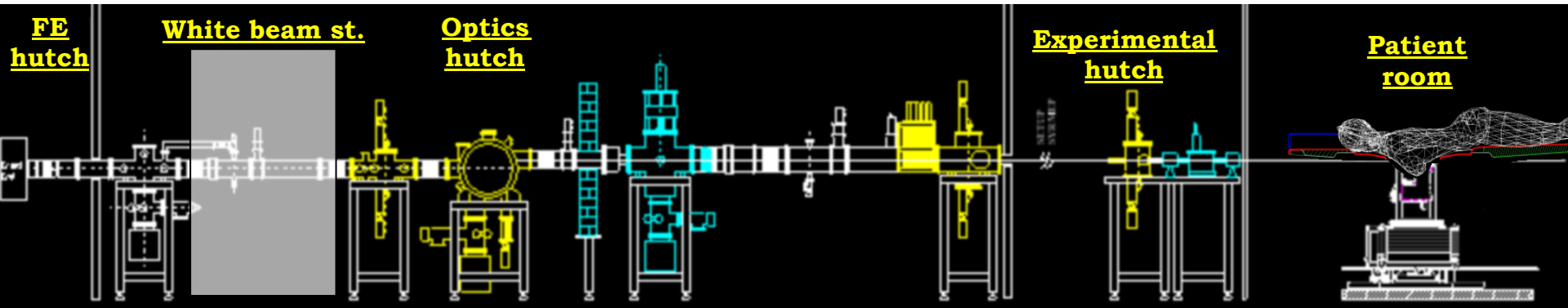
# Apparent absorption and refraction images



Apparent absorption



Refraction image



Not in scale!

- Front-end hor. acceptance: **7 mrad**
- Source-to-detector distance  $\approx$  **15 m** (white beam station),  $\approx$  **25 m** (exp. hutch),  $\approx$  **32 m** (patient room)
- Beam hor. size at sample  $\approx$  **10 mm** (white beam station),  $\approx$  **160 mm** (exp. hutch),  $\approx$  **210 mm** (patient room)
- Source size FWHM (h x v)  $\approx$  240  $\mu$ m x 90  $\mu$ m
- Energy range: **8.5 - 40 keV**, B.W.  $\Delta E/E \approx 2 * 10^{-3}$

## Techniques

- Absorption/Phase Contrast Imaging (free propagation)
- Dual energy imaging (K-edge subtraction)
- Analyzer Based Imaging (ABI)

*Modes:*

- *Planar*
- *Micro-CT*



Elettra  
Sincrotrone  
Trieste

# Breast imaging – first protocol with patients at Elettra

*Agreement among the Public Hospital of Trieste, the University of Trieste and Elettra*

**Aim:** Explore the potential of phase contrast imaging on selected cases

**Target:** Patients whose conventional diagnosis gave uncertain results.

**Modality:** I) PHC radiography with film systems  
II) PHC imaging with digital detectors  
III) Tomo-mammography  
(X-ray energy: 32-40 keV)

*Projection imaging*  
X-ray energy: 17– 22 keV

## Outcomes from the first protocol (I, II)

SR exams have:

- higher specificity,
- better agreement with the golden standard (biopsy),
- improved image quality,
- strong reduction of delivered doses.



UNIVERSITÀ  
DEGLI STUDI DI TRIESTE



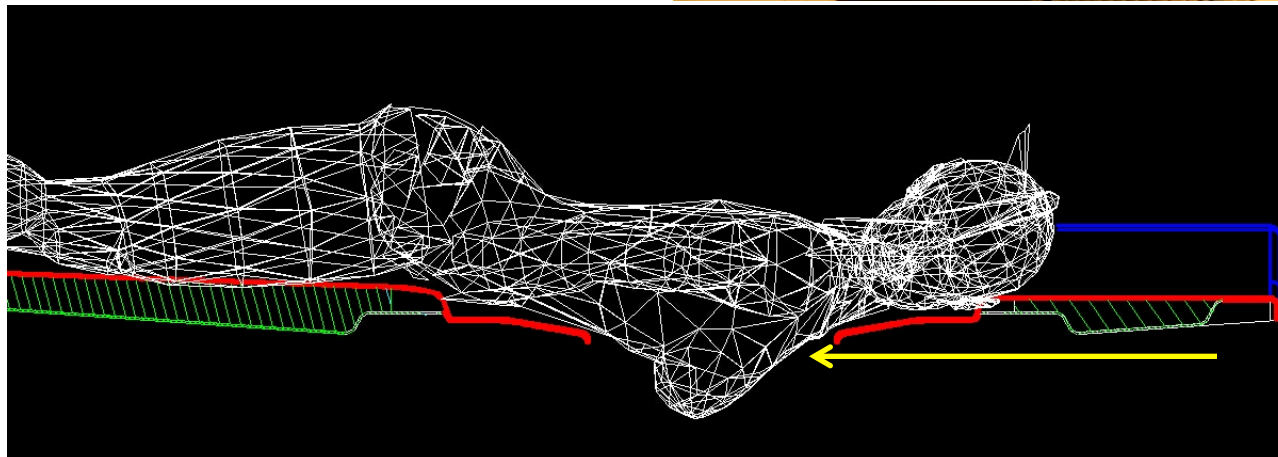
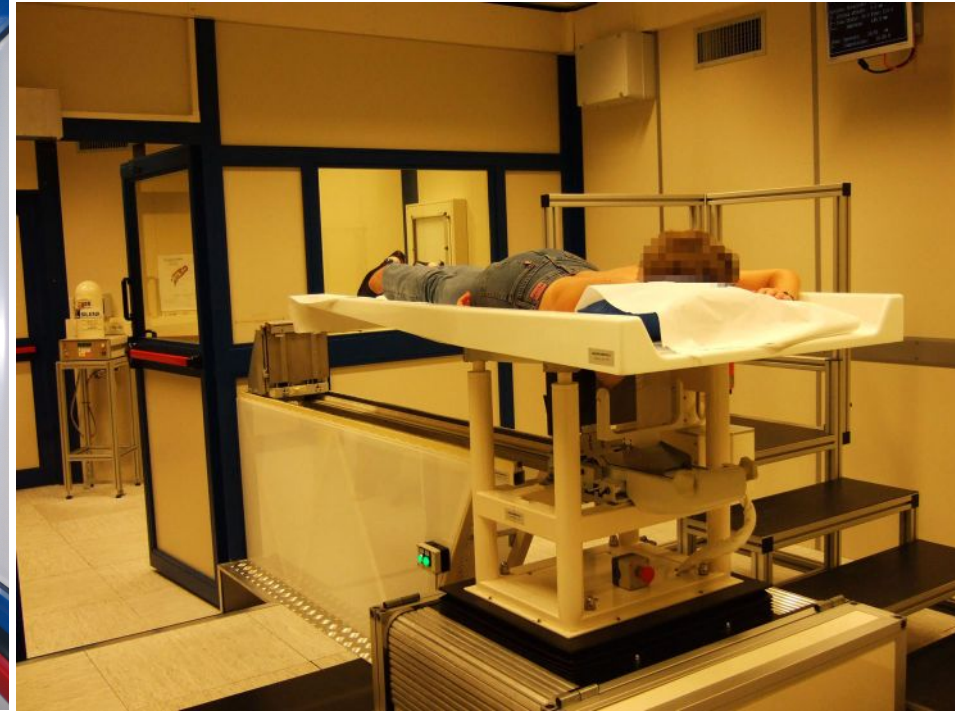
Fondazione  
FONDAZIONE CR TRIESTE



Elettra  
Sincrotrone  
Trieste

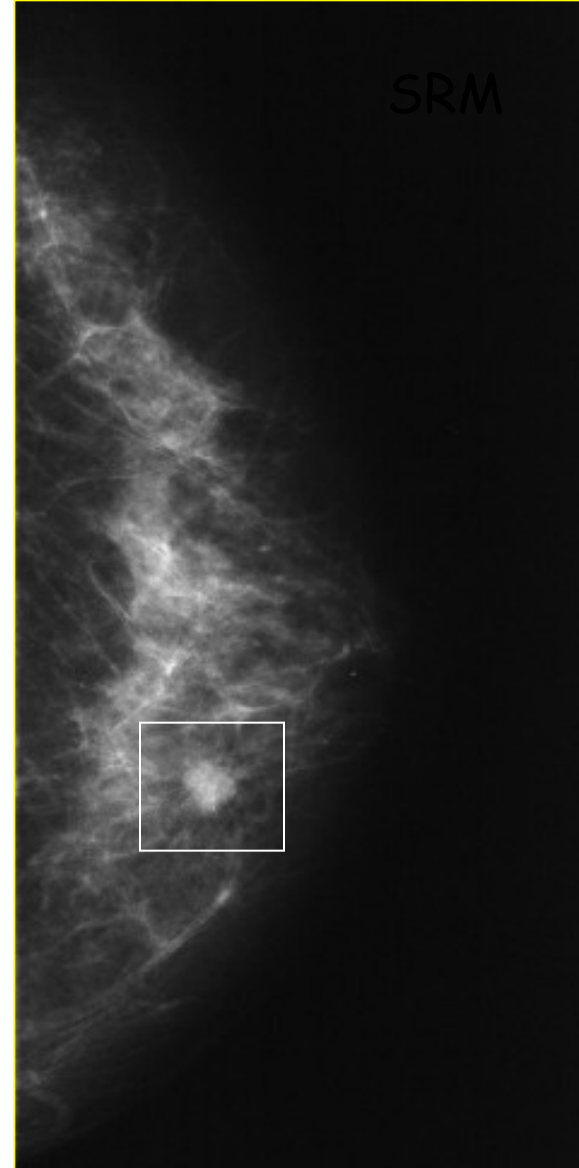
# Patient support

UNIVERSITÀ  
DEGLI STUDI DI TRIESTE





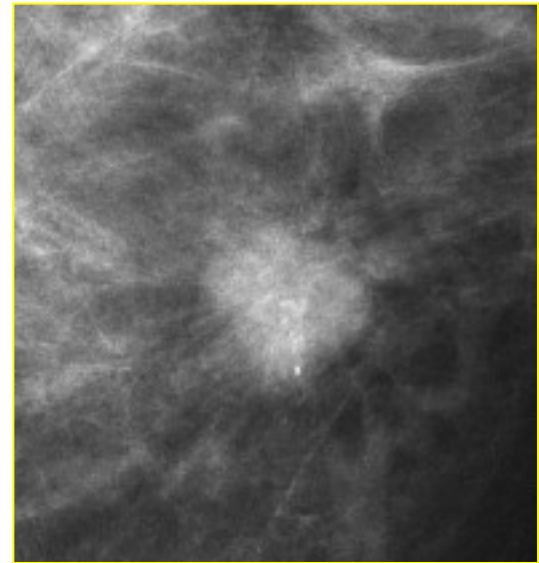
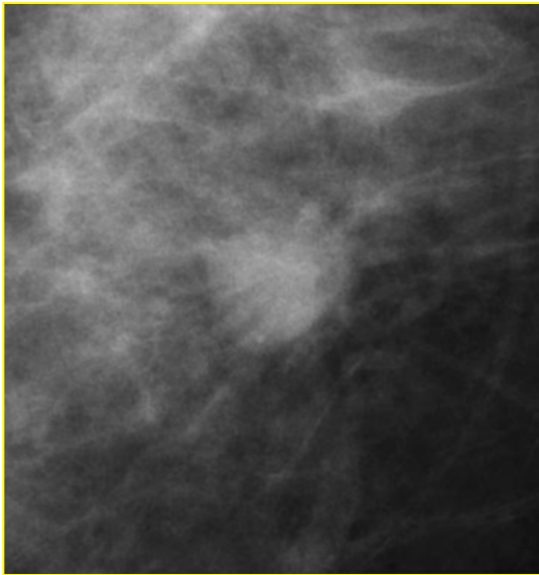
CONVENTIONAL unit



Synchrotron Radiation



Elettra  
Sincrotrone  
Trieste





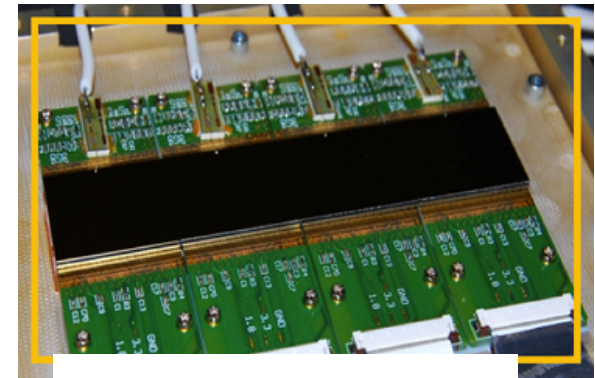
## Next-step: Tomo-mammography project (SYRMA-CT)

**Goal:** Design a new clinical protocol combining **planar projection mammography** and a **CT scan** (inline PHC) on a limited breast portion

**Diagnostic aim:** contribute to solve the cases of lesions overlap, improve the lesions characterization and visualize better their infiltration in the healthy tissue

**Key element:** CdTe single photon counting detector, 60  $\mu\text{m}$  pixel size, 25 $\times$ 2.5 cm<sup>2</sup> active area by PiXirad

Project financed by **Istituto Nazionale di Fisica Nucleare (INFN)**, Sections of: Trieste, Ferrara, Pisa, Napoli, Sassari



UNIVERSITÀ  
DEGLI STUDI DI TRIESTE



**Approval by ethic committee is needed**



# Main issues to be addressed

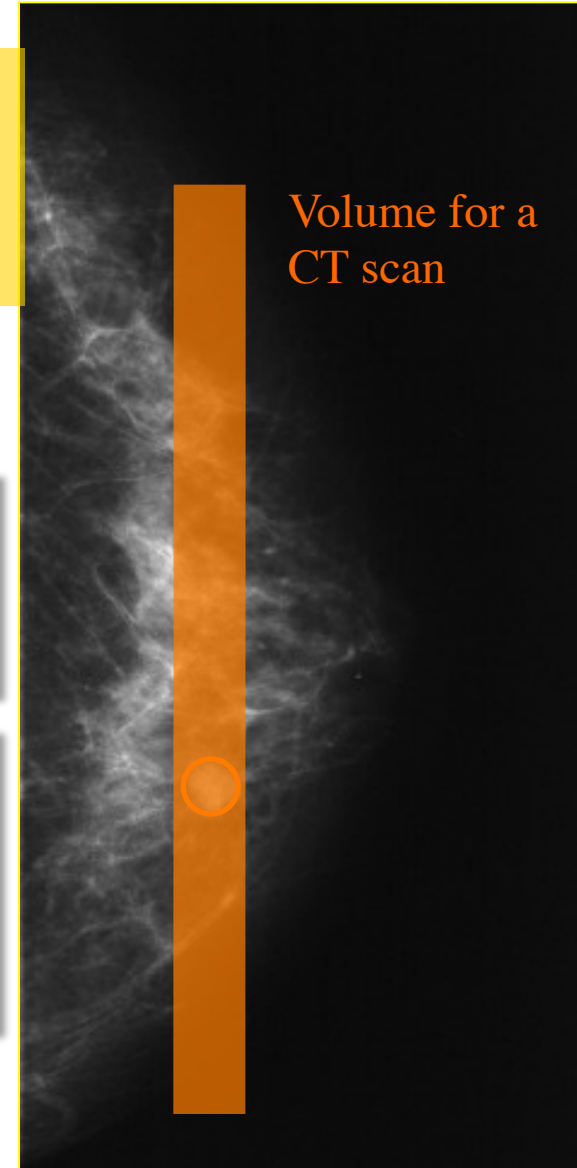
Exam procedure

- Identification of the region for the CT scan
- Choice of imaging parameters (X-ray energy, n. of projections, exp. time, etc.)
- Optimization of pre-processing and recon algorithms
- Post-processing
- *Dosimetry issues* and safety system upgrade
- Protocol implementation in the exam supervisor

- CT scan (~600 projections) must be performed at the same dose of a conventional examination (~5-10 mGy): feasible?
- Is *phase contrast* effective at high X-ray energy and with such low dose/projection?

## Phase retrieval algorithm (\*)

- Phase and amplitude extraction from a single distance image of a homogeneous object
- Refractive index:  $n = 1 - \delta + i\beta$   $\delta$ : phase shift term,  $\beta$ : absorption
- Transport of Intensity Equation (TIE) – Hom. phase retrieval algorithm
- Hom. Approx. : tissue as an homogeneous medium ( $\delta/\beta = \text{const}$ )



(\*)Paganin, D., et al., "Simultaneous phase and amplitude extraction from a single defocused image of a homogeneous object. Journal of microscopy, 206(1), 33-40 (2002).

# Low dose phase contrast breast tomography: optimization of reconstruction workflow

Combined experiments carried out at Elettra and at the Australian source with different detectors and energy ranges

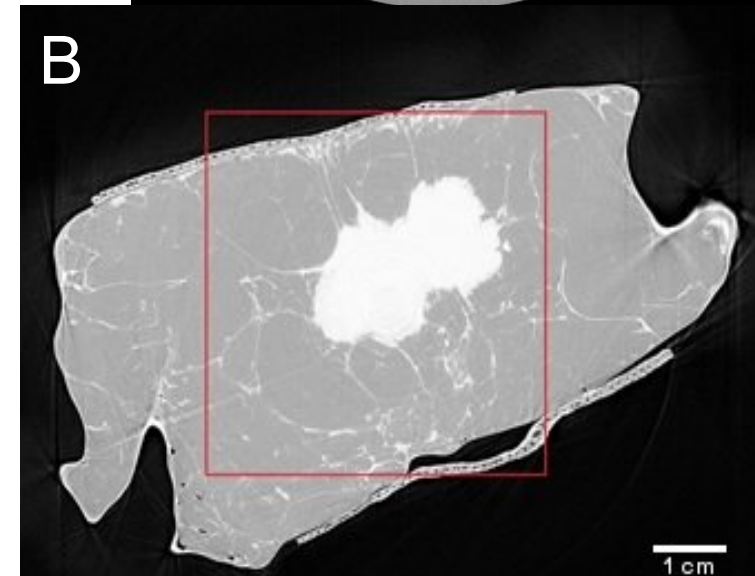
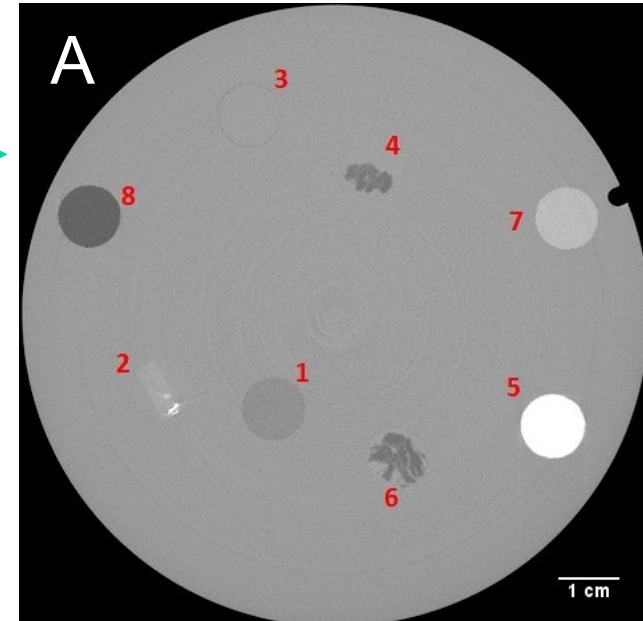
Geometrical test object and tissue specimens

CT in PB mode @ diagnostic dose (2.5 mGy AGD)

Reconstruction workflows  
Pre-processing, reconstruction, post-processing

Definition of image quality indexes & functions  
for comparison

Radiological Assessment



A) Polycarbonate phantom where 1 = Glycerol (C<sub>3</sub>H<sub>8</sub>O<sub>3</sub>), 2 = Unknown tissue (Malignant), 3 = Water (H<sub>2</sub>O), 4 = Fibrous tissue, 5 = Calcium Chloride (CaCl<sub>2</sub>), 6 = Adipose tissue, 7 = Paraffin wax, 8 = Ethanol (EtOH).

B) Reference image for the mastectomy sample reconstructed with FBP algorithm and considering 3600 high statistic projections. The red square indicates the region-of-interest used for the image quality assessment.



# Reconstruction workflows

Abbreviation	Phase retrieval	Reconstruction	Post-proc.
FBP	no	FBP	
FBP-ITER	no	FBP-ITER	
SIRT	no	SIRT	
SART	no	SART	
CGLS	no	CGLS	
EST	no	EST	
phr FBP	yes	FBP	
phr FBP-ITER	yes	FBP-ITER	
phr FBP-ITER Epan17	yes	FBP-ITER	Epanechnikov (w = 17)
phr FBP-ITER Susan5	yes	FBP-ITER	Susan (w = 5)
phr TV-MIN	yes	TV	
phr SIRT	yes	SIRT	
phr SART	yes	SART	
phr CGLS	yes	CGLS	
phr EST	yes	EST	

## Image quality indexes & functions

### Full-reference indexes (require a ref. image)

- MSE – Mean Squared Error
- SNR – Signal-to-Noise Ratio
- UQI – Universal Quality Index
- NQM – Noise Quality Measure
- SSIM – Structural Similarity Index

### No-reference indexes

- CNR – Contrast to Noise ratio
- FWHM – Full width half maximum
- Qs – Image quality characteristic(\*)

$$CNR = A_{feature}^{1/2} \frac{|\langle \beta_{lesion} \rangle - \langle \beta_{adipose} \rangle|}{[(\sigma_{lesion}^2 + \sigma_{adipose}^2)/2]^{1/2}}$$

$$Q_s = \frac{SNR_{out}}{F_{in}^{1/2} \Delta x}$$

- $F_{in}$  = incident photon fluence
- $\Delta x$  = spatial resolution of the imaging system
- SNRout = output signal-to-noise ration

(\*) T. Gureyev et al, Opt. Express 22, (2014)

### Radiological Assessment

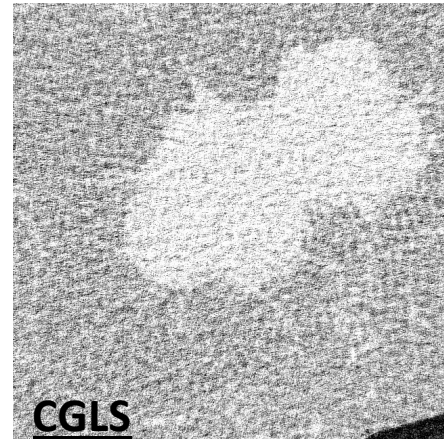
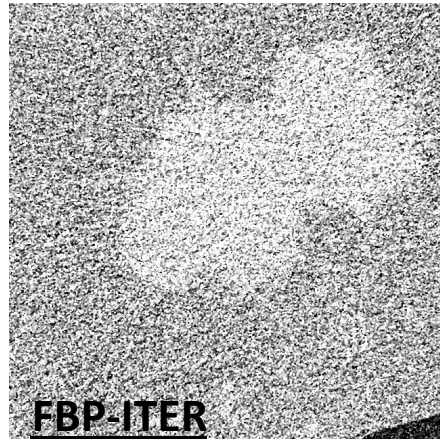
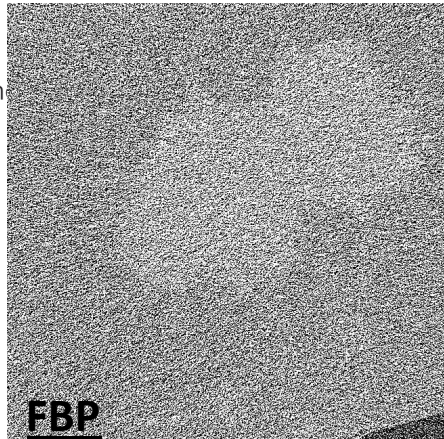
From 0 (worst case) to 4 (best image)

- No-diagnostic power (0 – 2)
- Poor diagnostic power (2 – 3)
- Full diagnostic power (> 3)

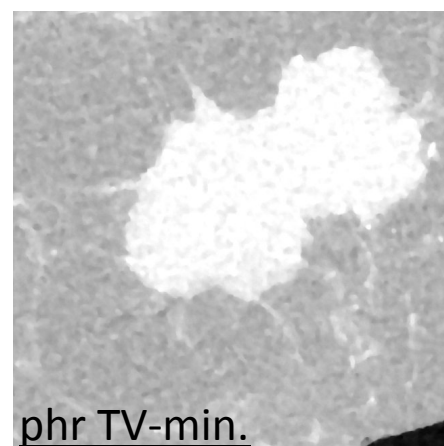
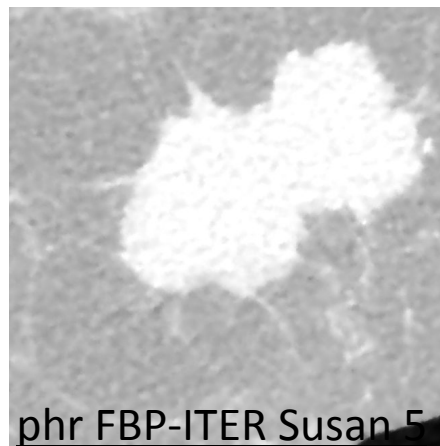
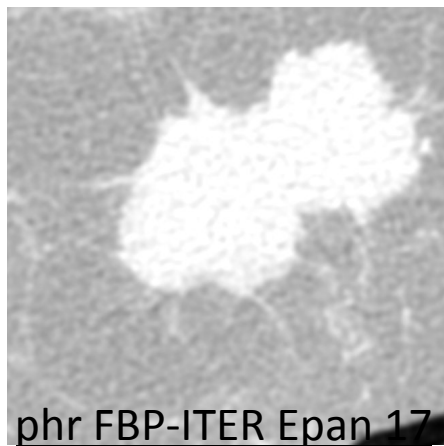


Elettra  
Sincrotron  
Trieste

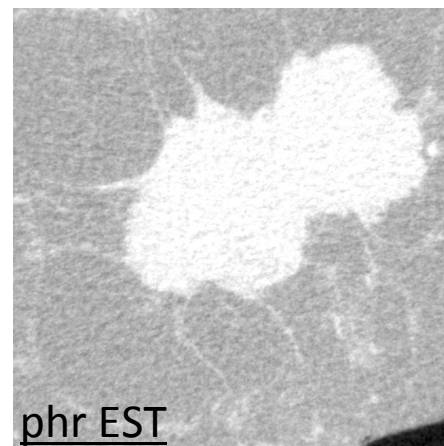
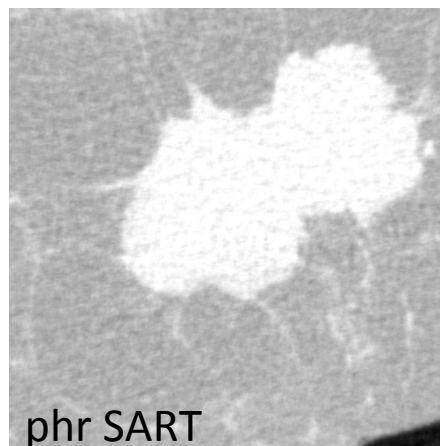
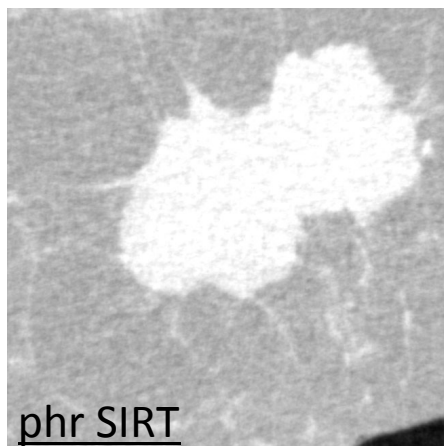
## NO- DIAGNOSTIC POWER



## POOR- DIAGNOSTIC POWER



## FULL- DIAGNOSTIC POWER



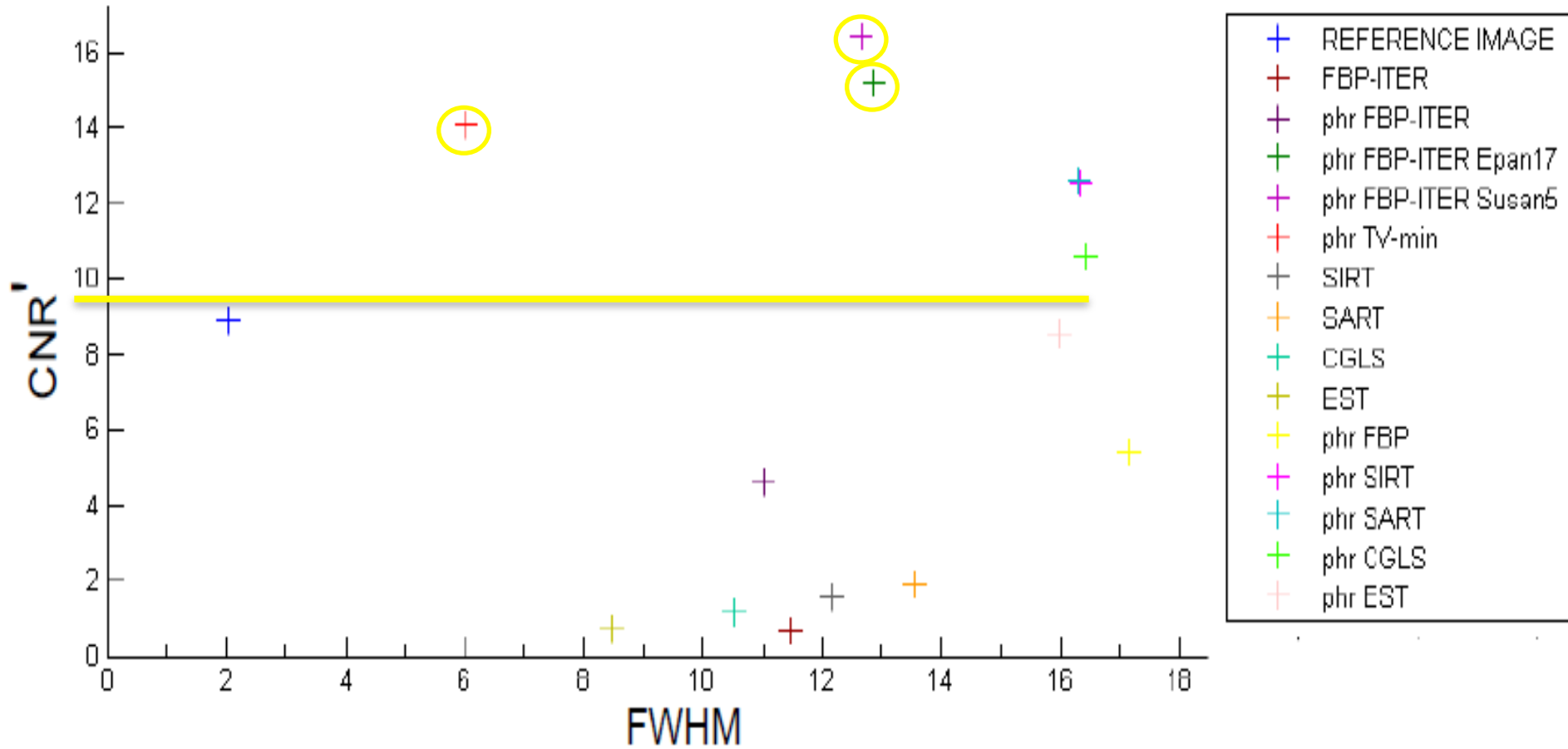
*S. Pacilè, et al: Biomed.  
Opt. Express 6 (2015)*

G. Tromba

ECSAC Conference Losinj, 2016



# Contrast-to-noise ratio and image *blurring*

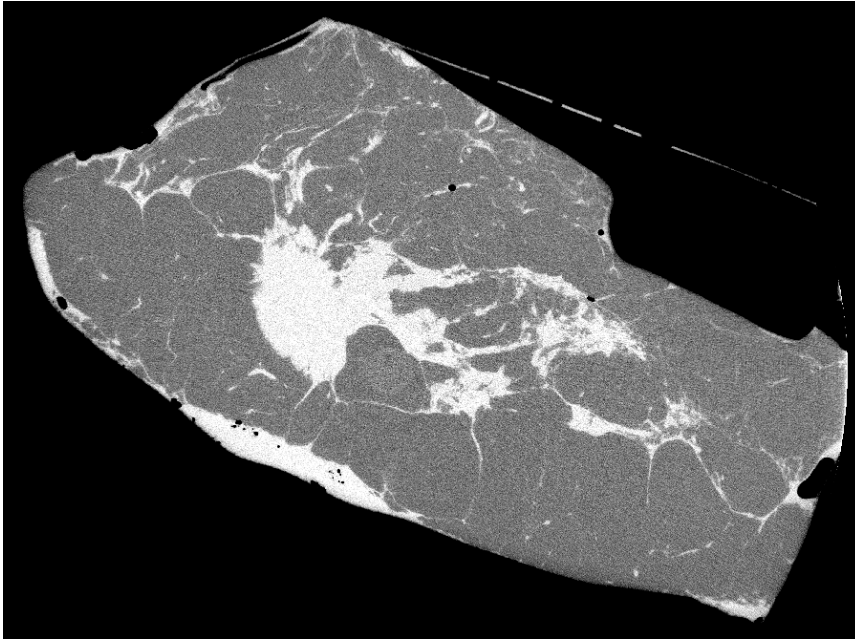


Full statistics ref image reconstructed with phase retrieval and FBP:  $CNR' = 30.5$ ,  $FWHM = 5.8$

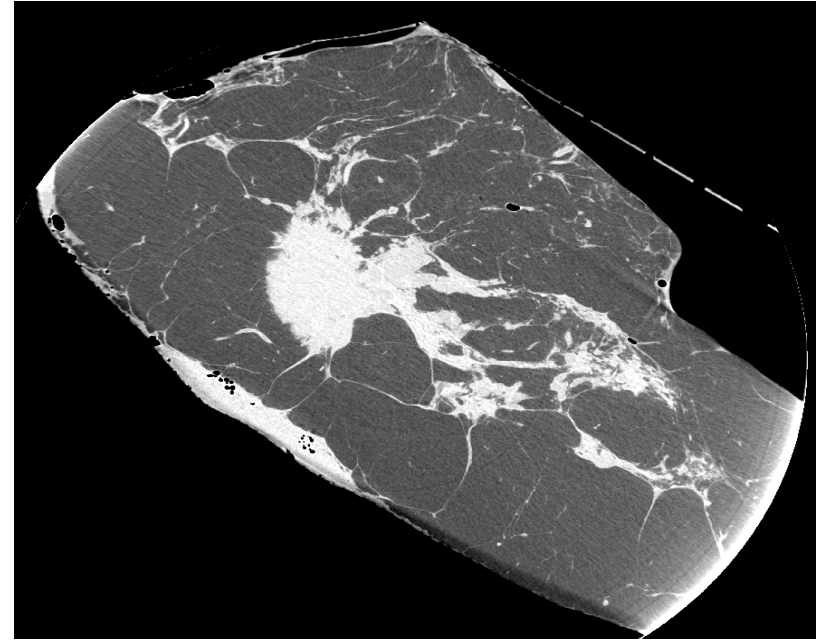
FWHM expressing image blurring is evaluated on the phantom images)



## Experiment at SYRMEP, Nov. 2015 – large propagation distance (9m)



Slice reconstructed from **high-dose CT (~20 mGy)** scan at 0 m propagation distance Hamamatsu detector



Same slice reconstructed from **low-dose (5 mGy mGD) PCT** scan at 9 m propagation distance Hamamatsu detector

E = 38 keV

Absorption and PB CT slice of a mastectomy sample with a tumour

Detector: Hamamatsu Flat Panel, pixel size = 100  $\mu\text{m}$



# Potentials of ABI

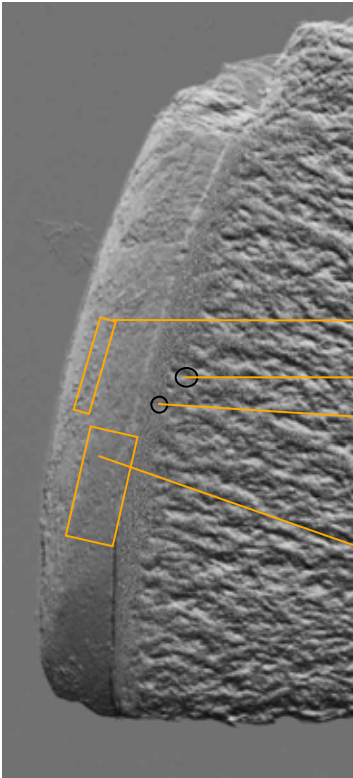
- Studies of cartilages and bones interfaces
- Imaging of finger joints





# ABI studies of Cartilage and bone interface

Osteoarthritis (OA) is a disease characterized by the progressive degeneration of articular cartilage and the development of altered joint congruency. It has a high incidence in the adult population. Affecting mainly the elderly population, it is one of the main causes of disability worldwide. Conventional radiography detects only **important osseous changes**, at advanced OA stage, when therapeutic strategies are less effective. **Early changes** in the **cartilage** and other **articular tissues** are **not** directly visible. MRI imaging works better but the maximum achievable spatial resolution is not always adequate.



Need to study:

- cartilage
- cartilage-bone interfaces
- changes in the bone structure

Superficial Layer (Zone of horizontal collagen fibers with flat cells)

Subchondral Bone Plate (**Important for diagnostic purposes in OA**)

Tidemark (Border between normal and mineralized cartilage)

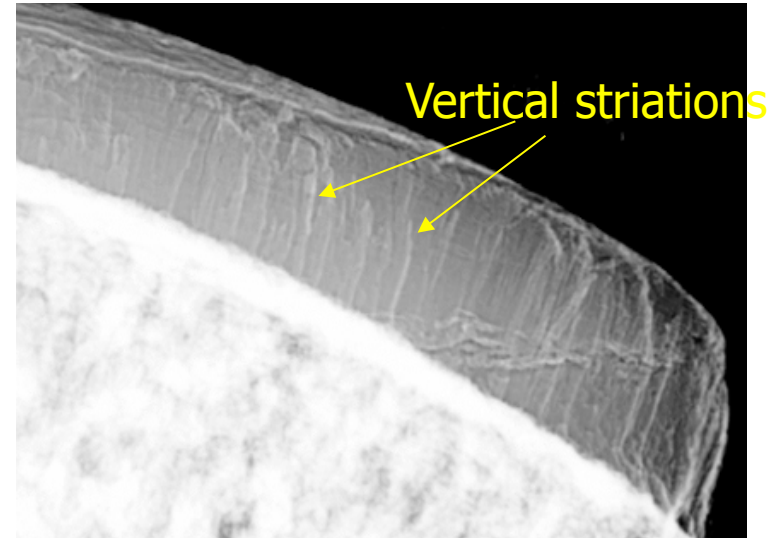
Transitional and Deep Layer (round cells, collagen fiber switches from horizontal to vertical orientation, increasing stiffness and material density)

**Aim:** detect the architectural arrangement of collagen within cartilage and evaluate how the cartilage degeneration affects the underlying subchondral and trabecular bone.

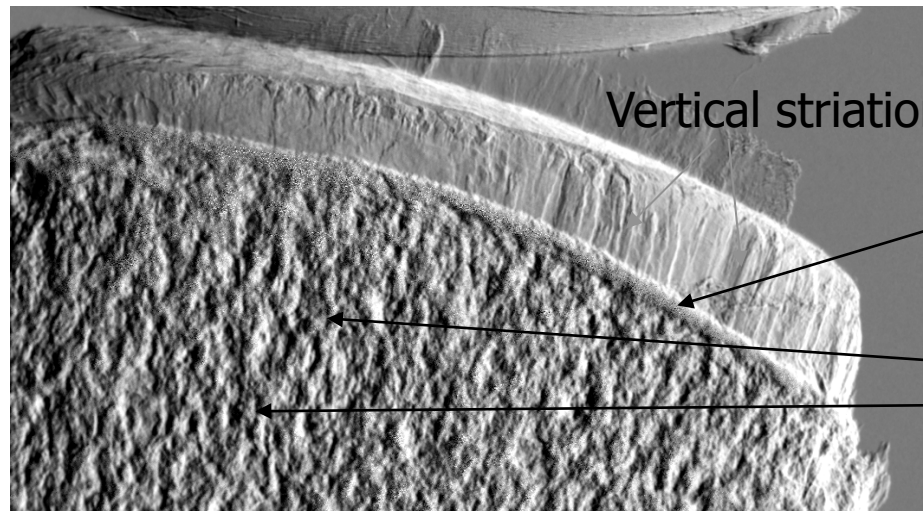


## Femur head core cuts: collagen arcades structure

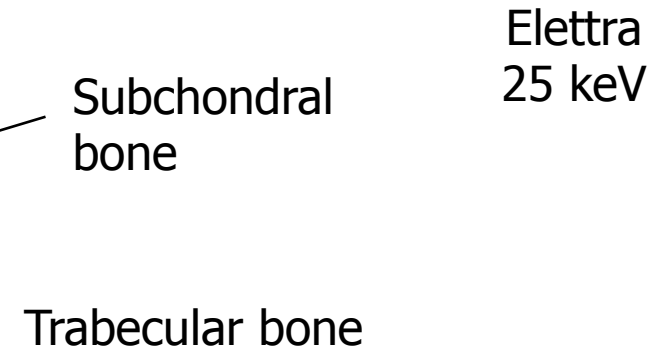
- The ABI technique allows to visualize the discontinuities in the sample and the inner structures invisibles by means of conventional X-Ray imaging.
- The transition bone-cartilage is emphasized.
- The articular cartilage striations are well visible due to X-ray diffraction at edges of fibers



### Refraction image



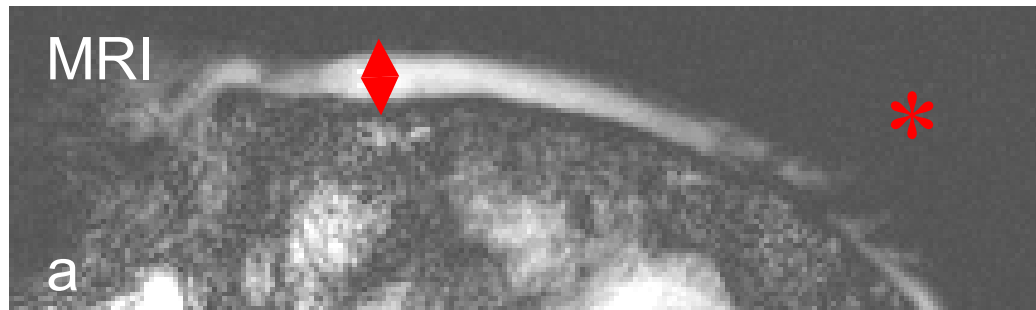
### Apparent absorption image



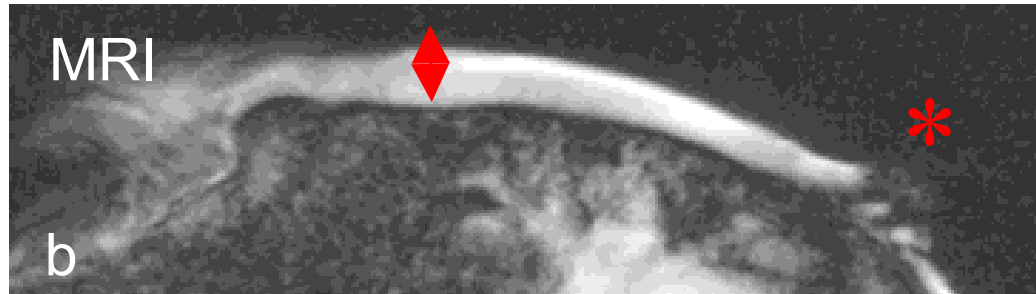
Muehleman C, et al., Osteoarthritis and Cartilage 12 (2): 97-105 FEB 2004



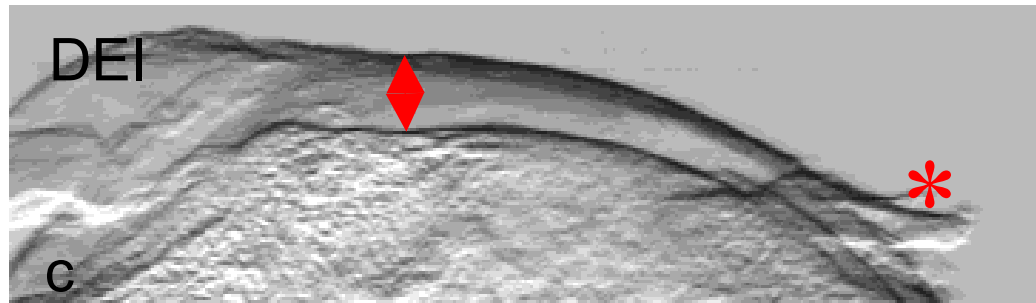
# Femur head core cuts: comparison with MRI



5 sec



150 sec



A Wagner, et al., Nucl. Instr. and Meth. in Phys. Res. Section A, 548(1), 47-53 (2005).



Elettra  
Sincrotrone  
Trieste

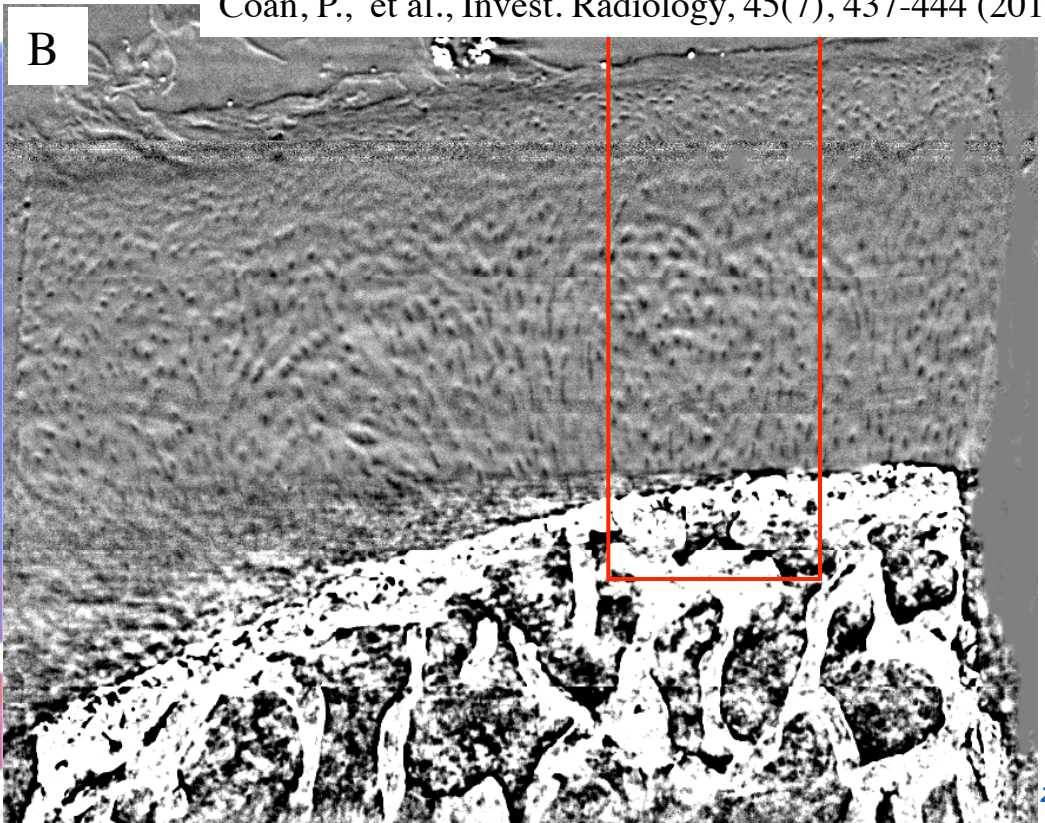
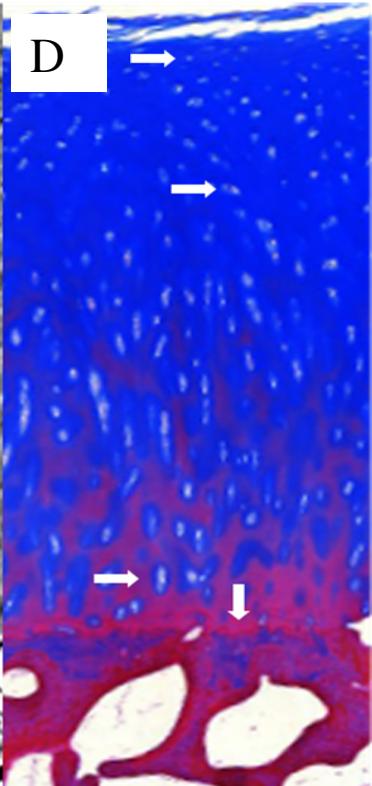
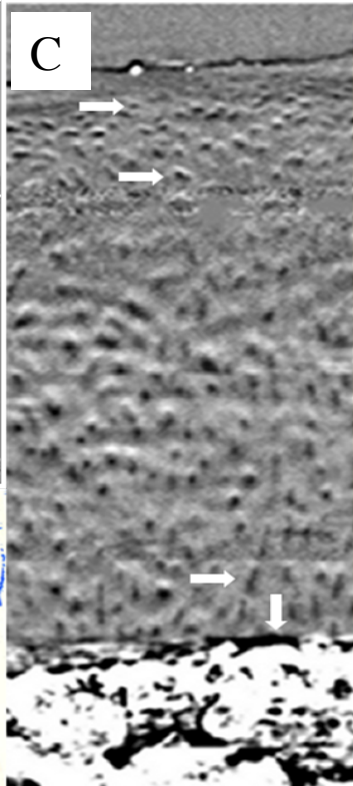
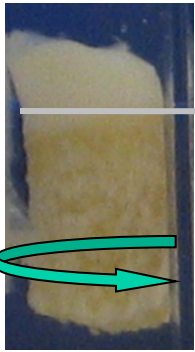


Specimen of normal cartilage (A), Coronal plane extracted from the reconstructed CT volume (B), Magnified portion identified by the ROI (C), Corresponding section from histologic preparation (D).

E = 26 keV, pixel size = 8 x 8 μm<sup>2</sup>.

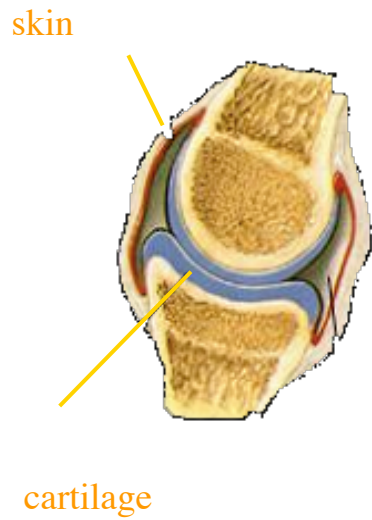
ABI in planar and tomographic modes was performed *in vivo* on articular joints of guinea pigs. Images showed the potential of technique in revealing initial lesions. Images with high spatial resolution and with an acceptable radiation dose.

A



Coan, P., et al., Invest. Radiology, 45(7), 437-444 (2010)

# ABI studies of the finger joint



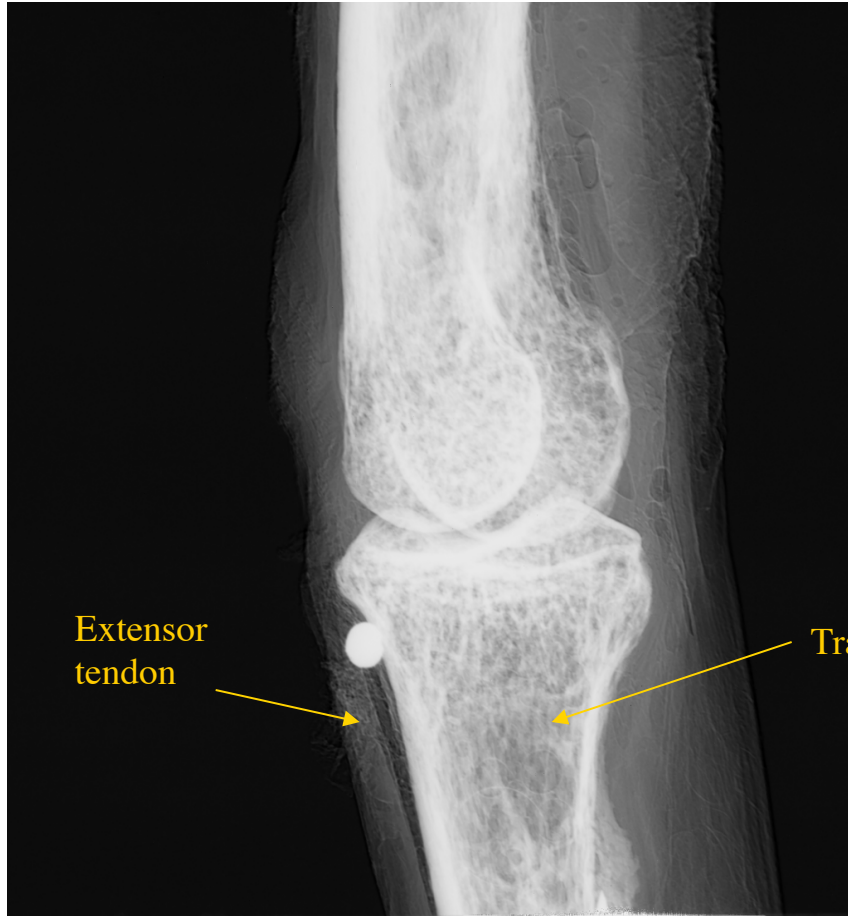
Conventional radiograph



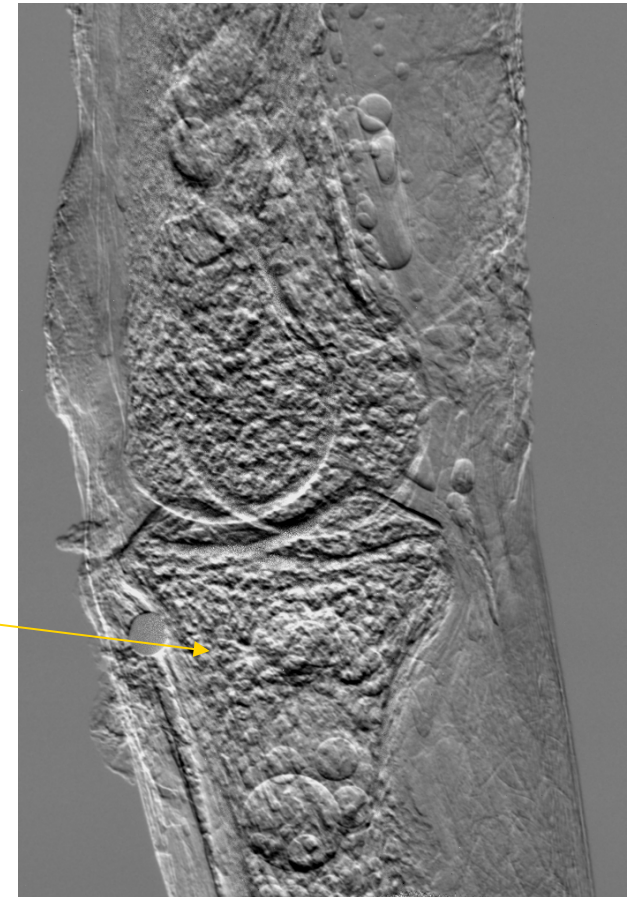
Apparent absorption image @ 20 keV  
at ELETTRA



# Index finger proximal interphalangeal joint

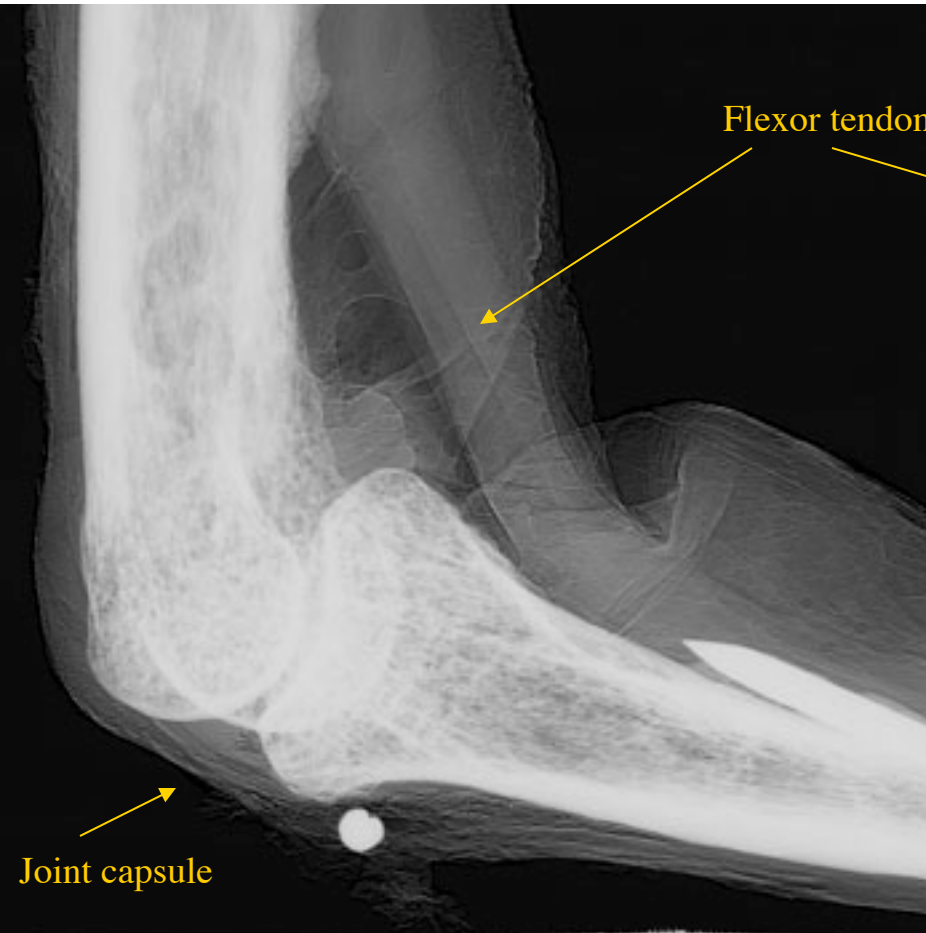


Apparent absorption Image

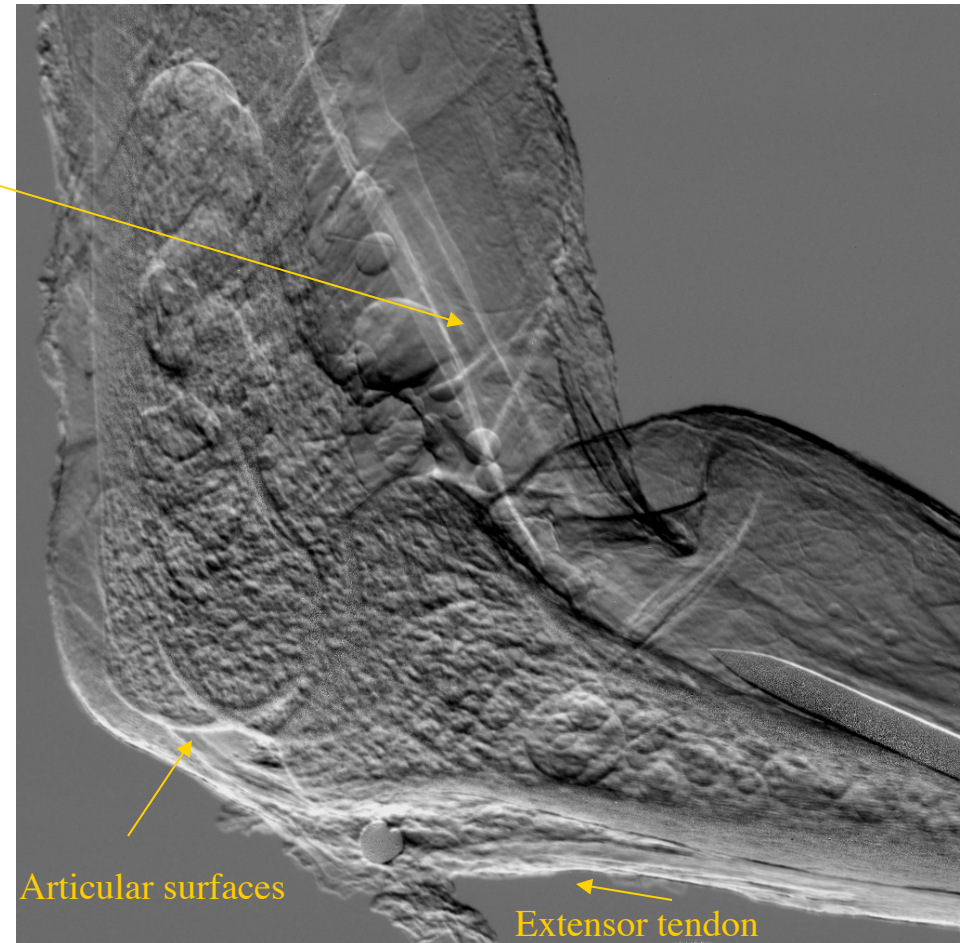


Refraction Image

# Index finger proximal interphalangeal joint



Apparent absorption Image



Refraction Image



# Lungs imaging

Techniques: Propagation based phase contrast

Modalities: planar for *in-vivo* images on rabbits  
ex-vivo micro-CT for a high resolution functional and morphological imaging of asthmatic mice





Elettra  
Sincrotrone  
Trieste

# In vivo studies at Spring 8 (Japan) Effects of Ventilation on Lung Liquid Clearance at Birth

Aim: to observe lung aeration on a breath-by-breath basis.

## Birth: a major physiological challenge

- ✓ Clear the airways of liquid
- ✓ Entry of air generates surface tension
- ✓ 10 fold increase in pulmonary blood flow
- ✓ Large increase in blood oxygenation
- ✓ Animal model used to study respiratory problems affecting pre-term borns.

- Animal model: rabbit pups
- Imaged pups with phase contrast imaging (FPI), either before the first breath (fetus) and at fixed intervals after birth (up to 2h)



MONASH University  
Science



Absorption Contrast

Phase Contrast, 25 keV, z=2 m



Lateral  
View



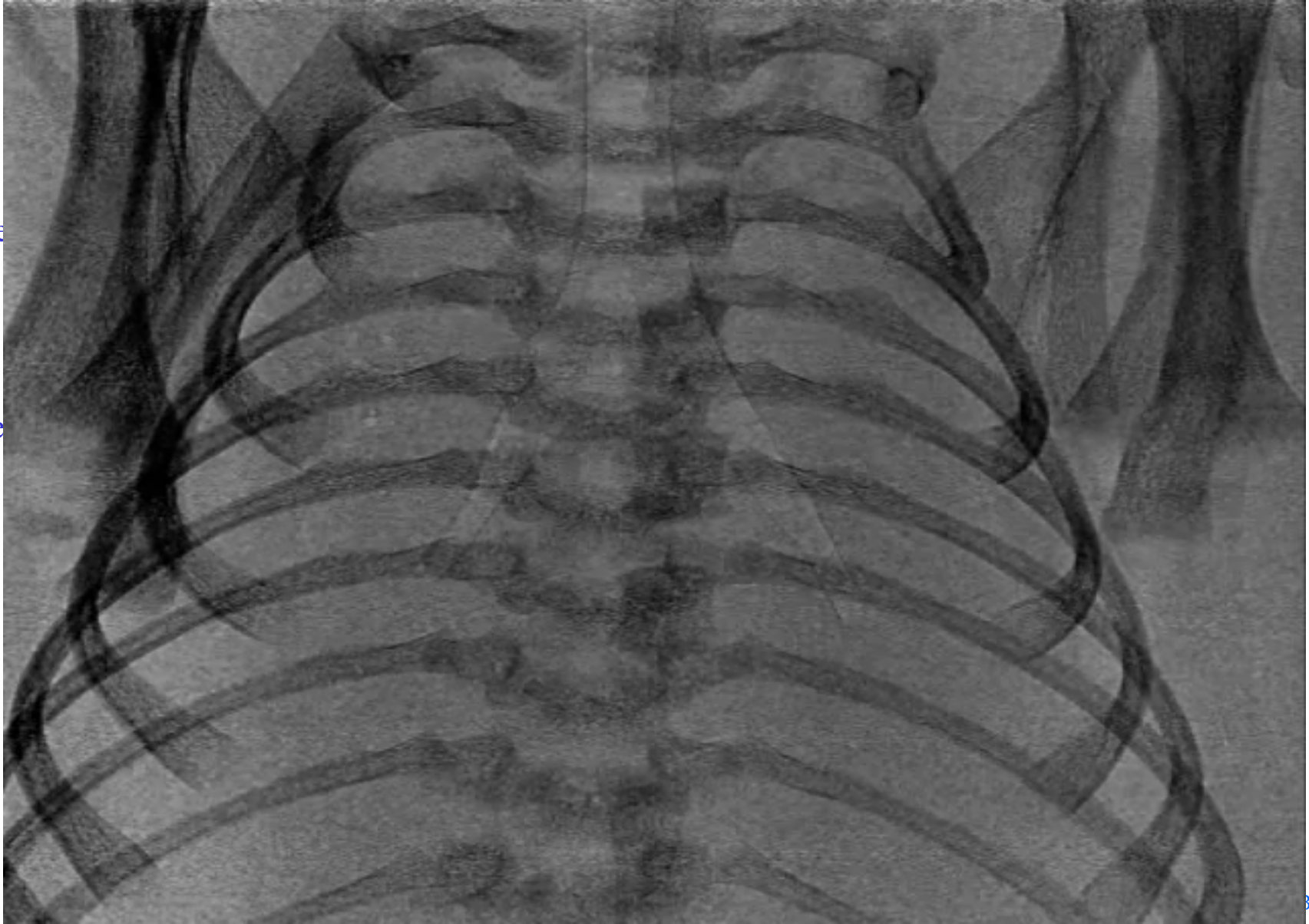


Exp. time:  
80 ms

Interval:  
0.8 s

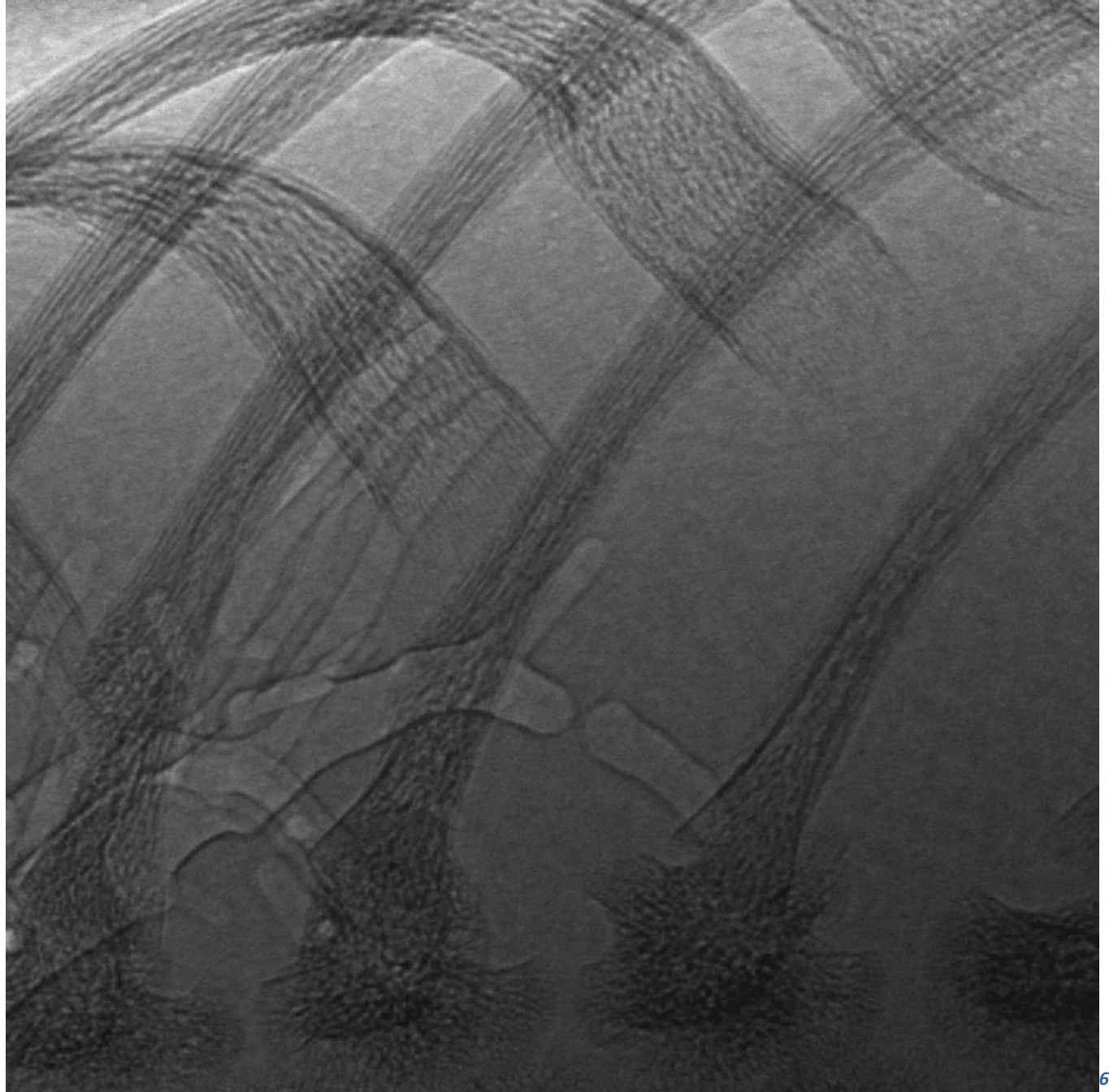
Skin Dose  
~ 0.15  
mGy  
per frame

Pixel Size  
22.5  $\mu\text{m}$





Elettra  
Sincrotrone  
Trieste

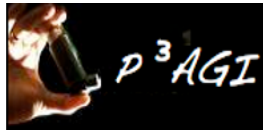




Elettra  
Sincrotrone  
Trieste

# Imaging of inflammation in asthmatic mice: combining functional and structural information

- Model of allergic asthma induced by ovalbumin based on balb/c mice developed by CBM in collaboration with the University of Wien.
- Aim: evaluate the potential of SR-based technique for **functional** and **morphologic** imaging of mice lungs
- Available techniques: optical imaging and PHC micro-CT
- Imaging protocol: tracking macrophages distribution
- Perspective for in-vivo studies (planar protocol within 2017 at SYRMEP (coll Goettingen – Incoming Talent3 project)



Public Private Partnership for  
Asthma Imaging and Genomics



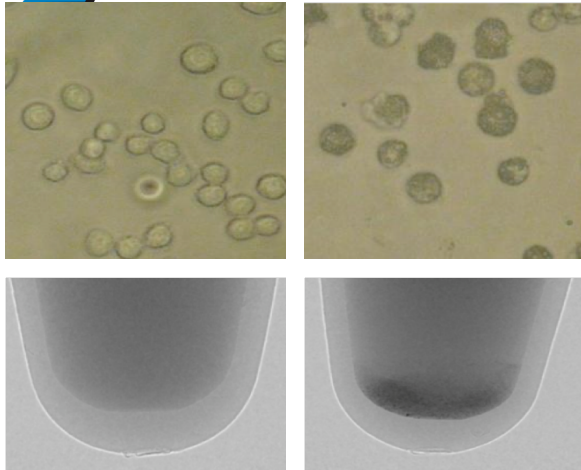
Linköping University



Programme on Scientific and Technological  
Cooperation between Italy and Sweden financed  
by Ministero degli Esteri



## Imaging protocol: use of macrophages with double staining



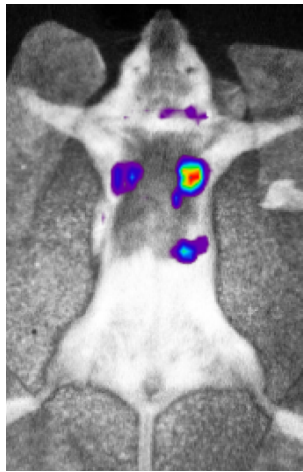
Unlabeled  
macrophages

Macrophages  
labeled with Ba

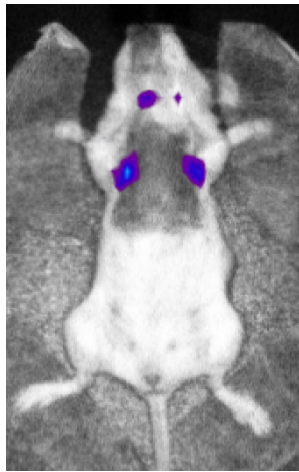
Use of immortalized Murine Alveolar Macrophage Cell line with double staining:

- **Barium sulfate** (clinical contrast agent Micropaque CT (Guerbet, F))
- **DiD fluorescent dye** to be used for cells localization inside the lungs using fluorescence microscopy.

Macrophages were administered intra tracheally 48 hours after asthma induction



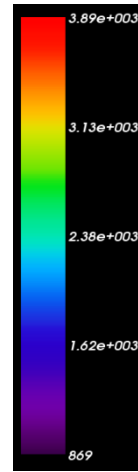
**Asthmatic** mouse  
treated with  
macrophages



**Normal** mouse  
treated with  
macrophages



**Native** mouse  
untreated

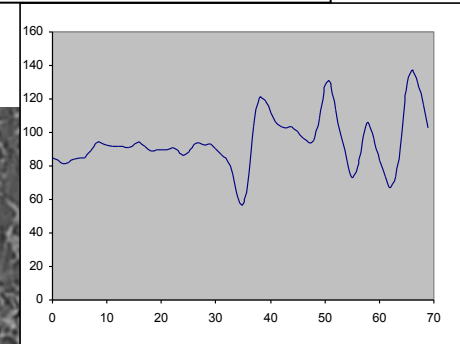
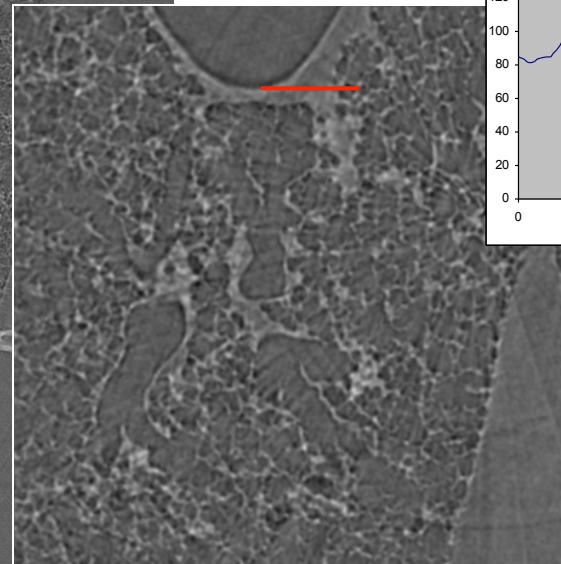
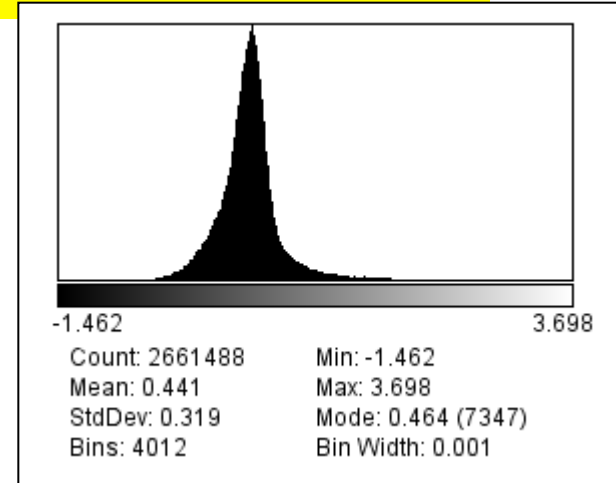
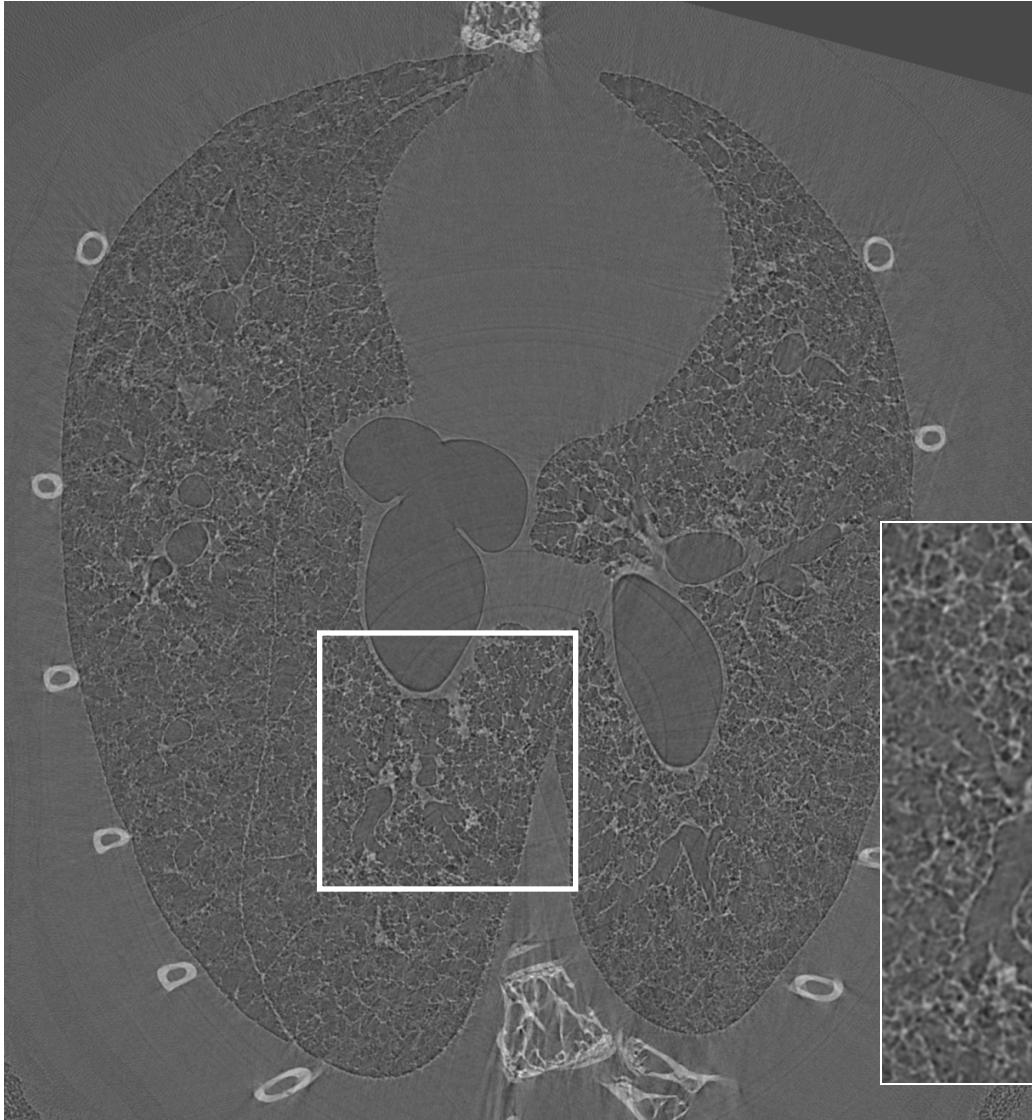


*In vivo* validation of homing of the macrophages to the inflammation sites.

Images performed 24 hours after macrophages administration.



# Reconstructed slice – Filtered back projection standard reconstruction procedure



**Typical edge  
enhancement effects  
due to phase contrast**



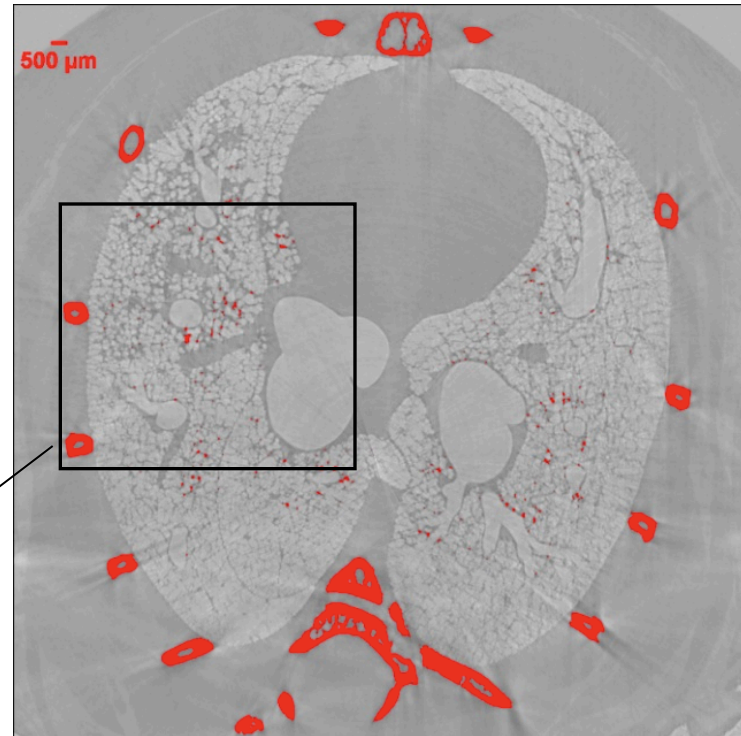


Sample: acute asthma mouse treated with macrophages labeled with Barium

*Phase Retrieval pre-processing algorithm is applied to CT projections, (prior to the reconstruction) to enable the decoupling of phase from absorption*

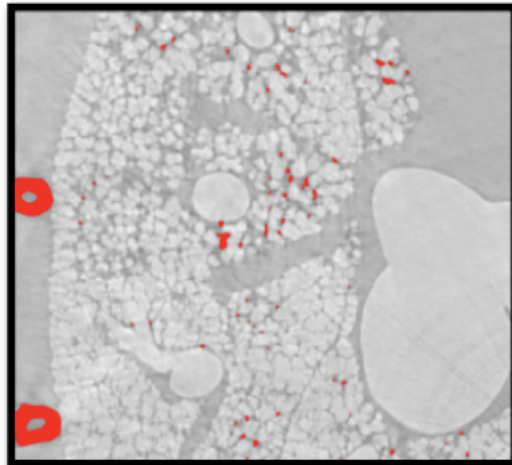
*Assumptions (Paganin et al., 2002):*

- near field phase contrast regime
- materials with  $\delta\beta = \text{const}$



E=22 keV  
PHC dist=30 cm

Bones  
Barium

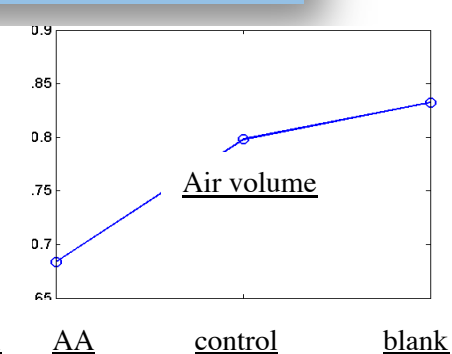
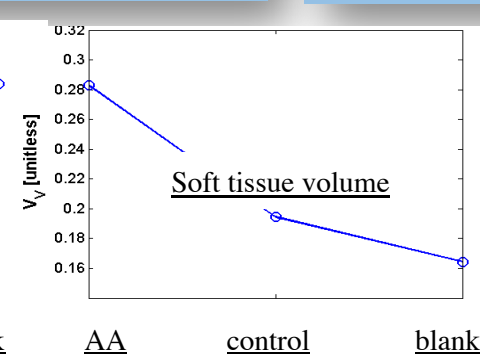
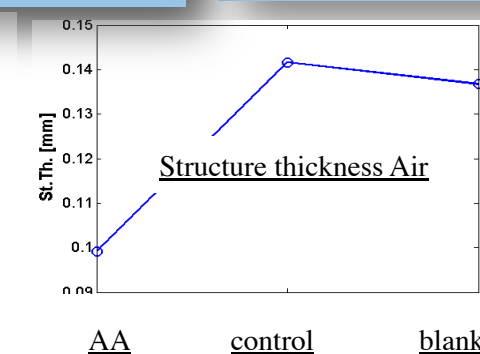
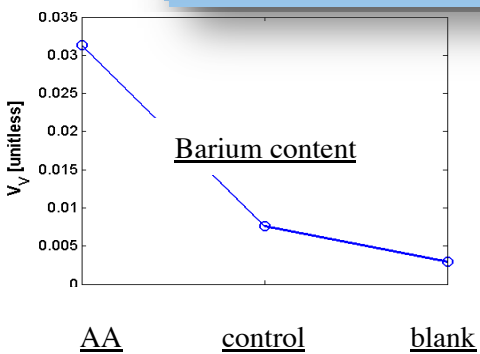
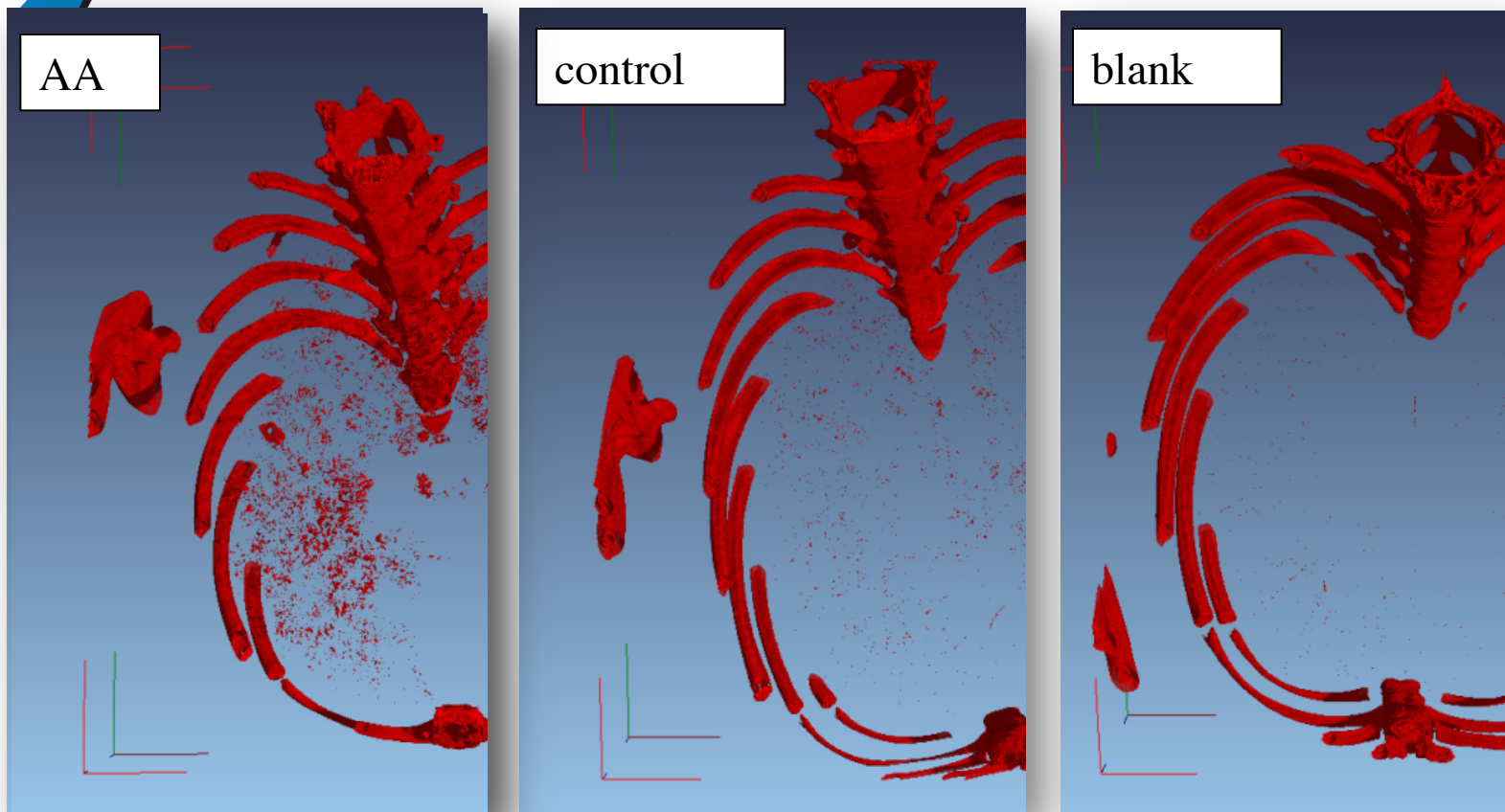


Application of Phase Retrieval for:

- Reducing the artefacts due to PHC effects around the tissue edges
- Reducing the noise
- Enhancing the phases separation

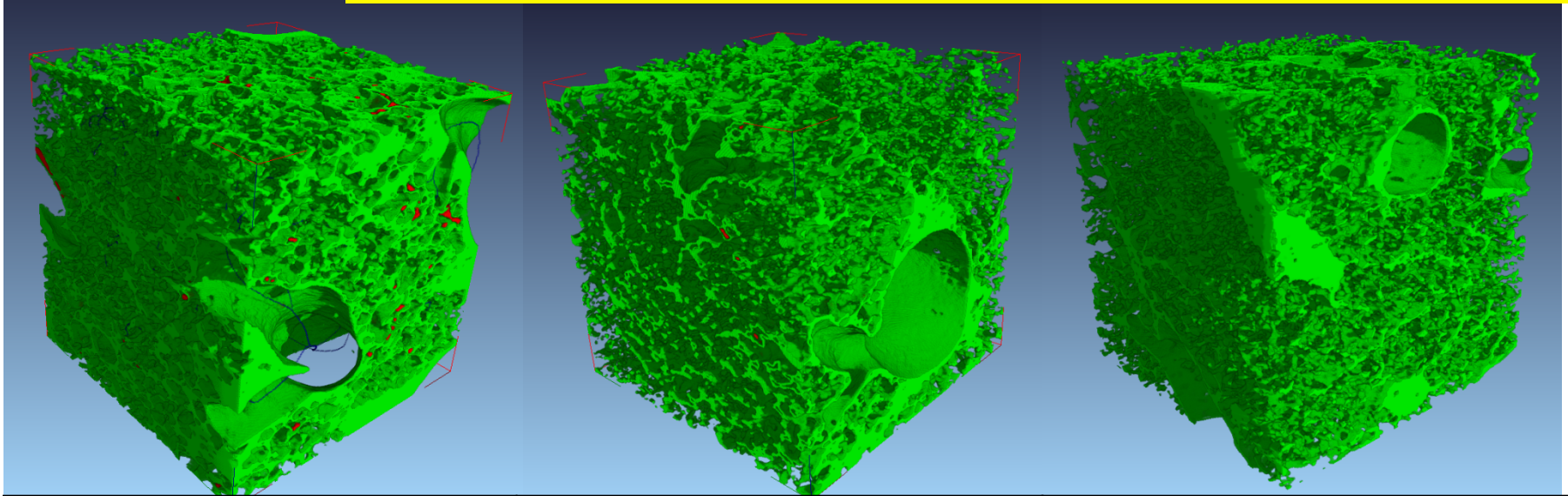


# Visualization of labeled macrophages



# VOI of soft lung tissue

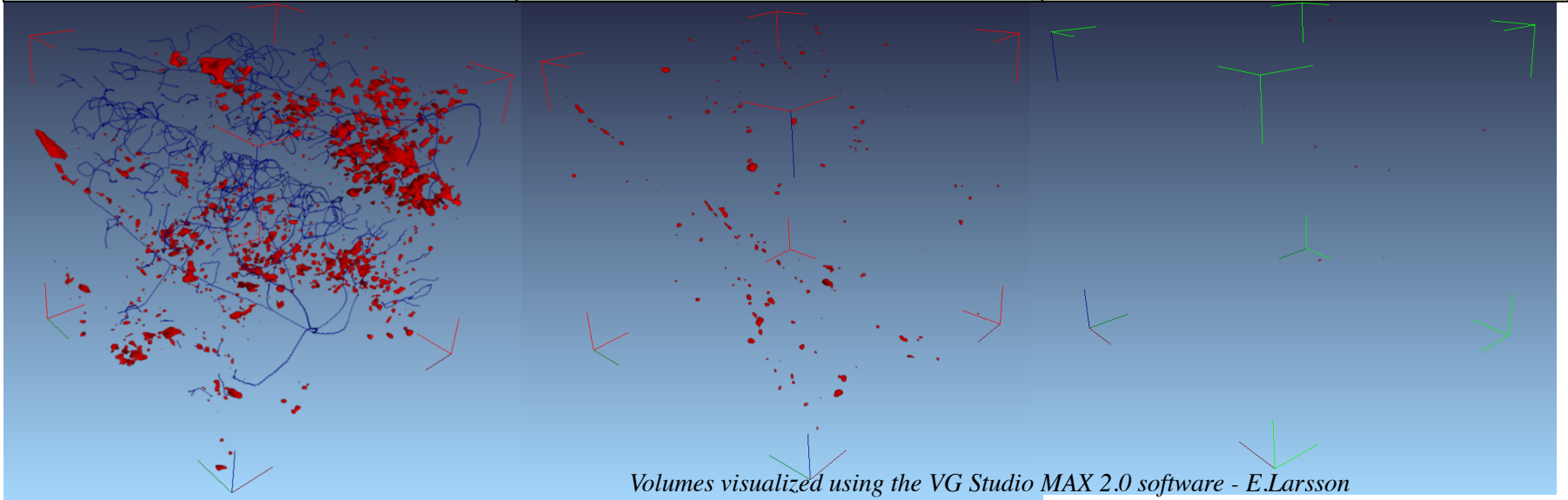
Soft Tissue (green), Macrophages with barium (red), Medial axis/skeleton (blue)



**a) asthmatic mouse treated with macrophages labeled by Barium**

**b) healthy mouse treated with macrophages labeled by Barium**

**c) control: healthy mouse untreated (no Barium)**



Volumes visualized using the VG Studio MAX 2.0 software - E.Larsson

# Cell tracking studies for imaging of brain tumors in rats

Glioblastoma multiforme (GBM) is the most common and most aggressive primary brain tumor in humans.

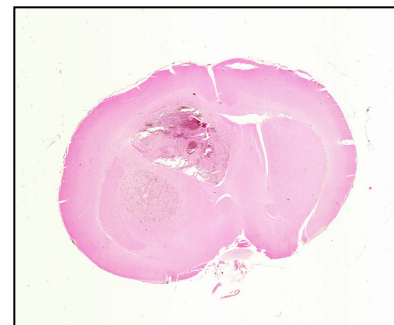
An animal model based on Wistar rats have been developed to study the behavior of the tumor and to monitor the effects of therapies.

Requirements for the cell tracking technique:

- to monitor the dynamic of tumour growth
- to follow the migration of tumour cells
- to understand the dynamic of metastasis spread



Section of healthy rat brain

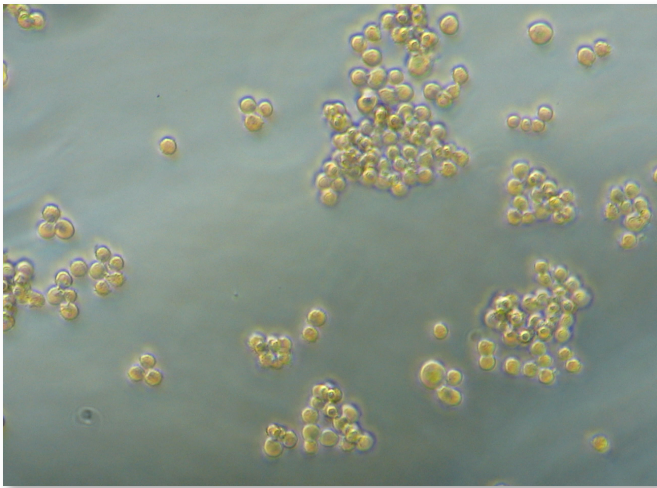


Section of rat brain with C6 glioma 2 weeks after implantation

C6 glioma cells were cultured and some of the cultures were exposed to colloidal Gold Nano Particles (GNP) for 22 hrs before harvest.

C6 glioma cells were implanted into the brain of adult male Wistar rats. The implantation was performed with the animals under general anesthesia. The animals were allowed to recover after the end of the implantation and were sacrificed two weeks later.

The detection of labeled cells is enhanced by the higher absorption of gold with respect to tissue and by PHC effects.



Gold Nano particles (GNP)

Our biological approach: Label tumor cells with sufficient Au nano particles (  $\text{\AA} \sim 50 \text{ nm}$  )

Inert GNP bond to serum proteins

GNP are taken up by phagocytosis stored in lysosomes and are not released by exocytosis

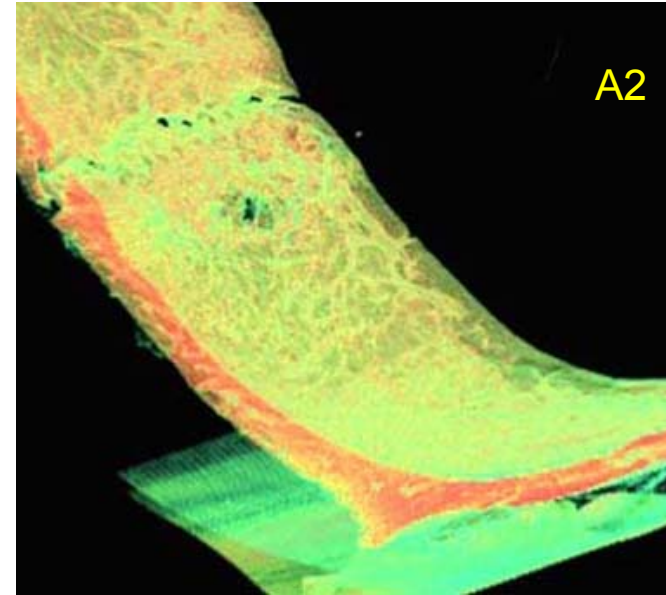
*Courtesy of E. Schultke, R.H.Menk et al.*



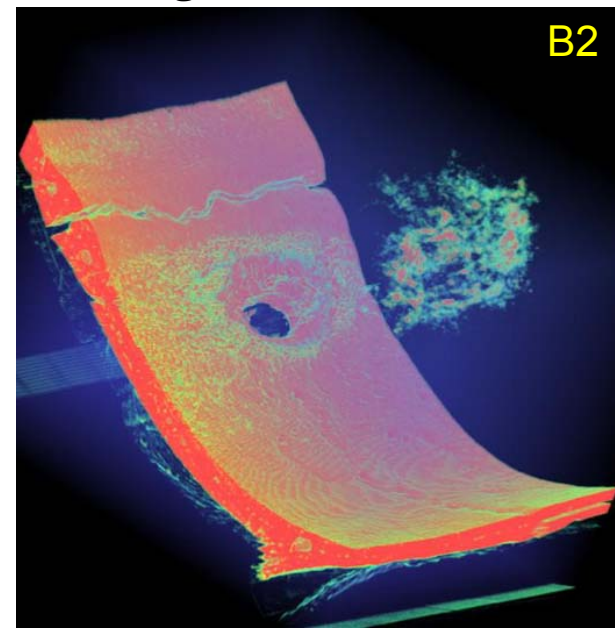
### A 1 and A 2: Tumor without colloidal gold

**3D rendering of a  
4 mm thick  
volume**

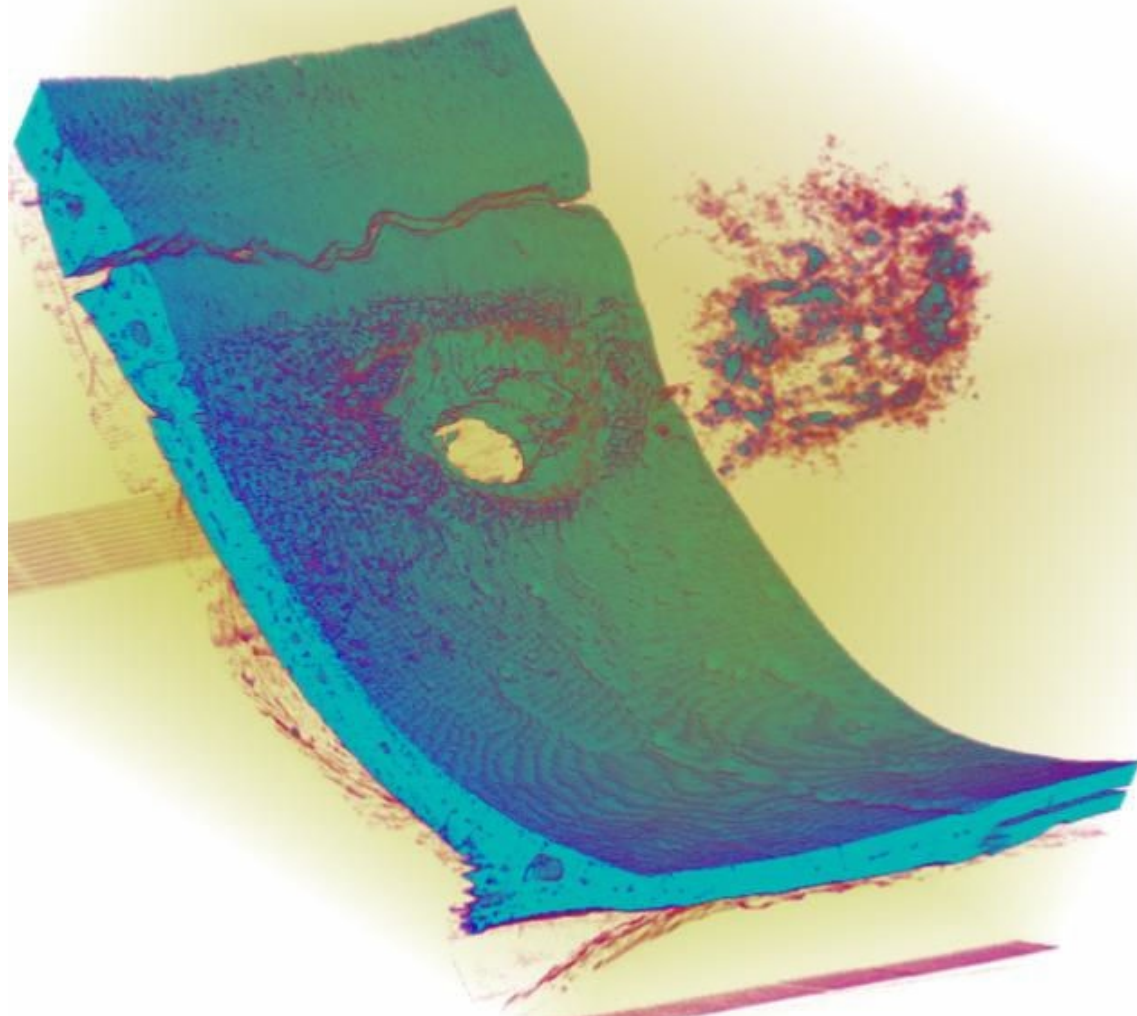
E = 24 keV  
Num. proj. = 720  
Pixel size = 14 $\mu$ m



### B 1 and B 2: Tumor with 300,000 colloidal gold-loaded cells



Courtesy of E.  
Schultke,  
R.H.Menk et al.

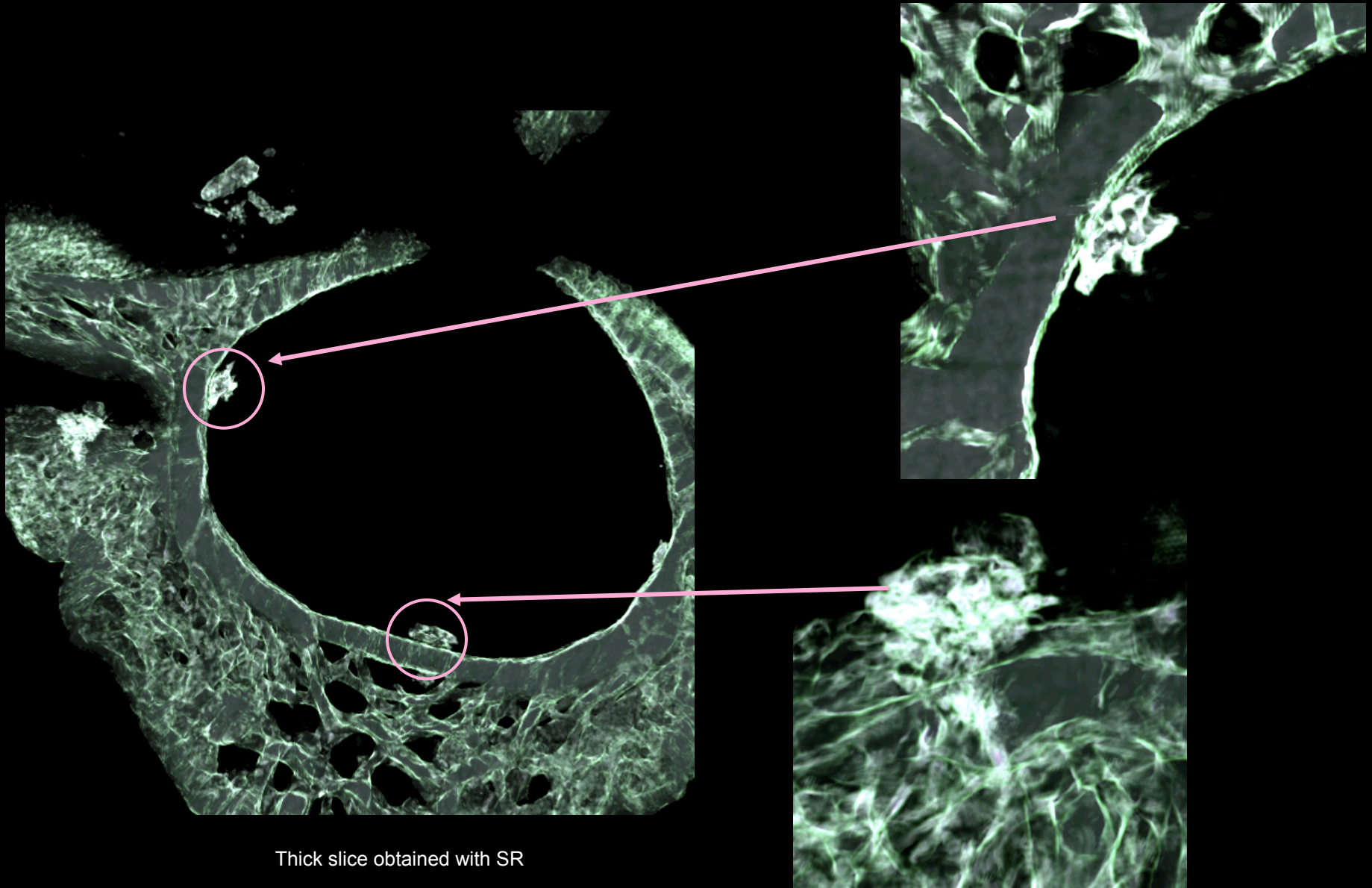


Rat 7, 100000 gold loaded C6 cells, 14 days incubation



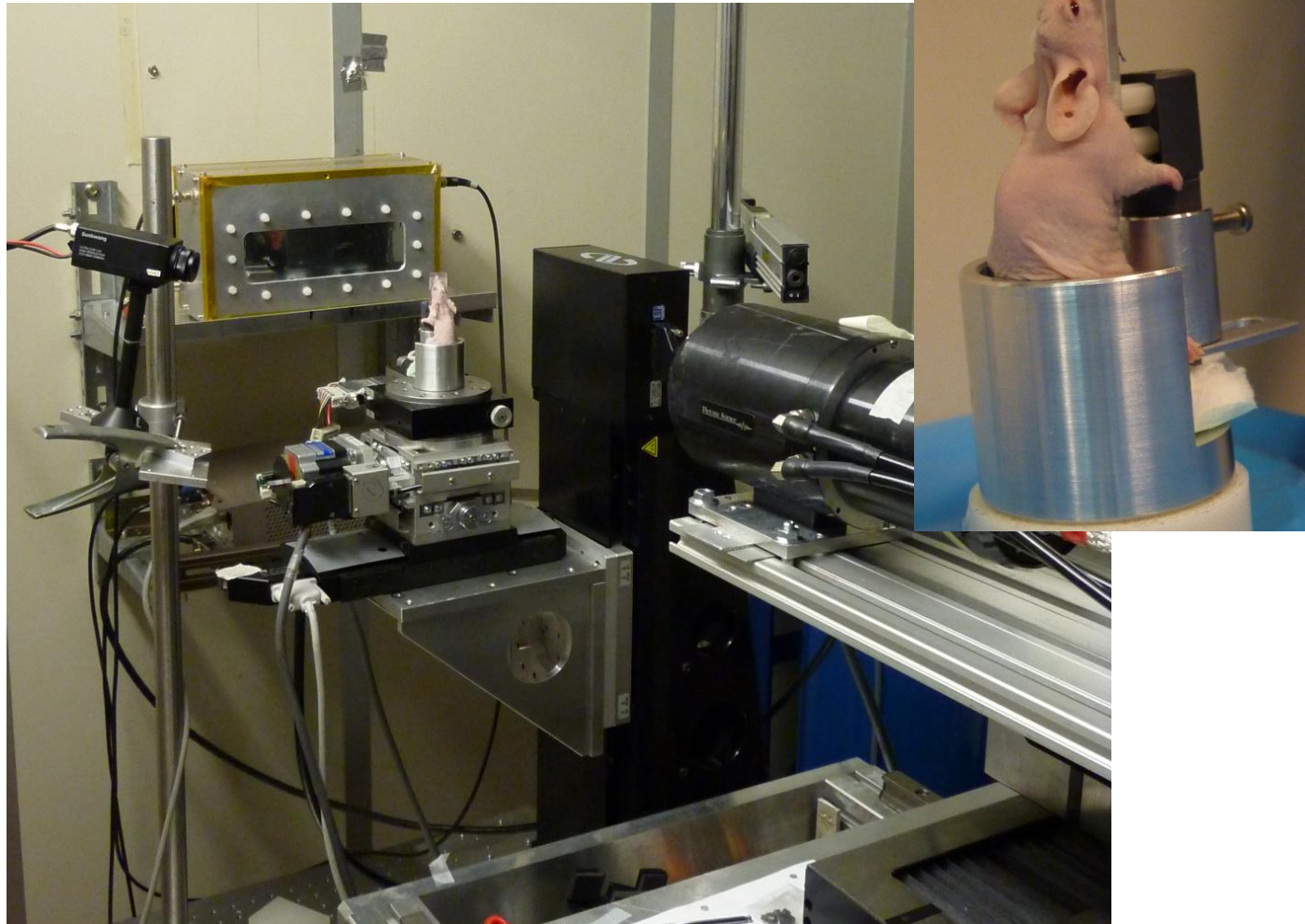
# Rat 706: Metastasis spread in the spine

Elettra  
Sincrotrone  
Trieste

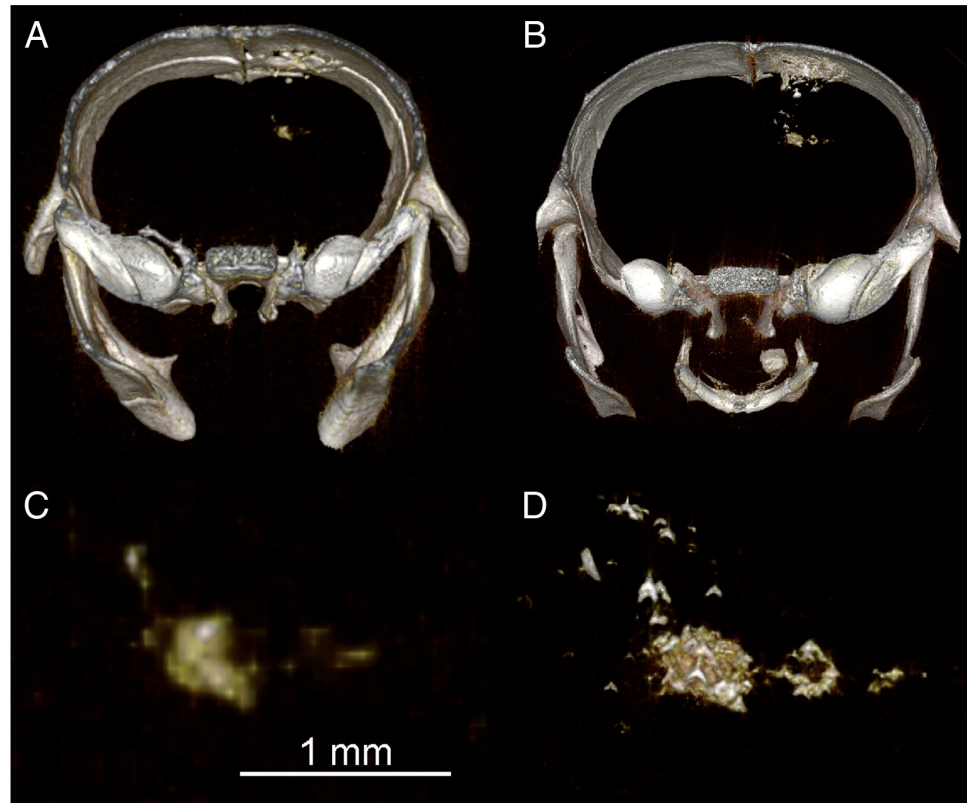


Thick slice obtained with SR





First experiment *in vivo* performed in Nov. 2010: lesions are visible also a low doses



- Comparison of two 3D renderings of a CT of a mouse injected with 100,000 GNP-loaded F98 cells depicts (A–C) the low x-ray dose in vivo data and (B–D) the high x-ray dose ex vivo data. The images in panels C and D are enlargements at full system resolution of the developed tumor depicted in panels A and B, respectively.





# Bone turnover in mice exposed to micro-gravity conditions

- 3 wild type (WT) mice and 3 pleiotrophin-transgenic (PTN-Tg) mice in a special payload (MDS - Mice Drawer System). The transgenic mouse strain over-expressing pleiotrophin (PTN) in bone was selected because of the PTN positive effects on bone turnover.
- **91 days in the International Space Station (ISS) by NASA: Aug. - Nov. 2009.**
- Controls:
  - mice on Earth in the same special payload MDS (*ground* mice)
  - mice in common cages (*vivarium* mice)
- SR  $\mu$ -CT experiments were performed on femurs and spines
- Being non-destructive,  $\mu$ -CT is very attractive for these rare specimens



University of  
Genova



Università Politecnica delle  
Marche

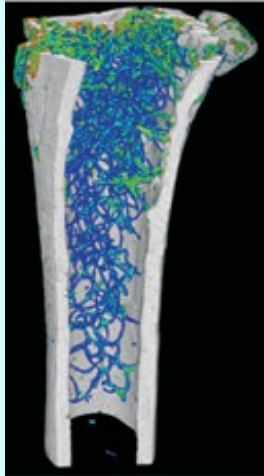


University of Trieste – Dept. of Engineering

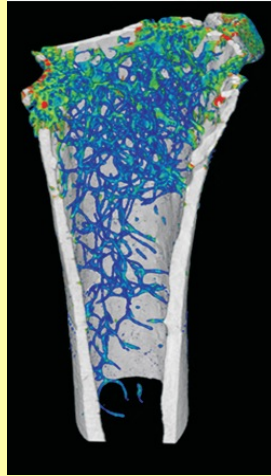


# Analysis of the microarchitecture of the trabecular bone in femurs

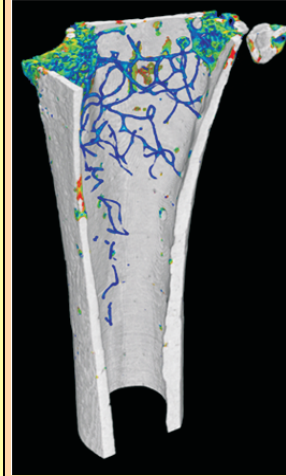
VIVARIUM



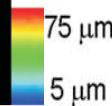
GROUND



FLIGHT



WT2



Revealed:

- a **bone loss** during spaceflight in the weight-bearing bones
- a **decrease** of the trabecular number
- an **increased** mean trabecular separation
- no significant change in trabecular thickness.
- No effects on not weight-bearing bones.

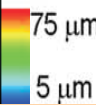
E = 19 keV

Pixel size = 9 μm

N. Proj = 900

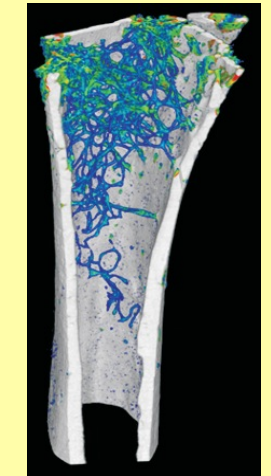
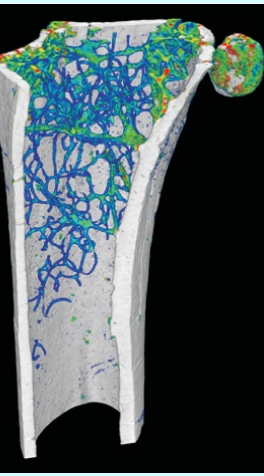
Distance sample-ccd= 3 cm

PTN-Tg2



Comparison WT vs.PTN-Tg2:

- PTN-Tg exposed to normal gravity has a poorer trabecular organization than WT mice
- the expression of the PTN gene during the flight resulted in some protection against microgravity's negative effects.



Color map represents bone trabecular thickness distribution in the femur (red = 75 μm, blue = 5 μm)



## Final considerations

It is worldwide recognized phase contrast imaging represents a revolutionary tool in bio-medical imaging

Besides PBI and ABI, in the last years, other phase sensitive techniques, like:

- Crystal and grating based Interferometry;
- Coded aperture methods,

have been developed, offering new opportunities for soft tissues imaging

Many efforts are directed to export these techniques to laboratory and clinic environment, either developing innovative experimental setup, and new generation sources ( $\mu$ -focus, compact synchrotrons, etc)

*giuliana.tromba@elettra.eu*

*Thanks for your attention*

